#5

SACLANTCEN MEMORANDUM
serial no.: SM-277

SACLANT UNDERSEA
RESEARCH CENTRE

MEMORANDUM

Performance assessment of the SACLANTCEN vertical array in shallow water

A. Bassias

March 1994

Page count for SM-277 (excluding Covers and Data Sheet)

Pages	Total
i–vi	6
1–50	50
	56

SACLANT Undersea Research Centre
Viale San Bartolomeo 400
19138 San Bartolomeo (SP), Italy

tel: 0187 540 111
fax: 0187 524 600
telex: 271148 SACENT I

NORTH ATLANTIC TREATY ORGANIZATION

SACLANTCEN SM-277

Performance assessment of the SACLANTCEN vertical array in shallow water

A. Bassias

The content of this document pertains to work performed under Project 02 of the SACLANTCEN Programme of Work. The document has been approved for release by The Director, SACLANTCEN.

Issued by:
Systems Research Division

R. Weatherburn
Division Chief

intentionally blank page

Performance assessment of the SACLANTCEN vertical array in shallow water

A. Bassias

Executive Summary: The problem of assessing both the performance of a vertical array of hydrophones during and after at-sea experiments, as well as the quality of the experimental data collected, is an important one. Although the performance assessment of the SACLANTCEN towed array is well-documented, similar documentation for the vertical array is not available. Such an assessment is useful to the Centre's various groups and also to people who work with vertical arrays. The SACLANTCEN vertical array is a line array of 64 hydrophones spanning a water column of 62 m. Before any actual experiments take place, the SACLANTCEN Signal Processing Group devotes several hours to array testing, using well-defined test signals, in order to have a rough assessment of the array's physical condition and functionality. In spite of this at-sea testing, the data collected generally need some further quality assessment to determine whether they would be suitable for use in other important tasks such as source localization or transient signal detection.

In this memorandum the performance of the SACLANTCEN vertical array is assessed, based on an analysis of experimental data collected in shallow water during the October–November 1991 Signal Processing Group sea trial. Certain measures have been used for the assessment of the performance of the array, as well as for the evaluation of the quality of the data, for both the signal and noise fields. These measures, although not unique, seen from the signal processing and statistical points of view, constitute a method that leads to the conclusion as to whether the array performed as expected both qualitatively and quantitatively.

Throughout this study, the signals received at the array – which were test signals – have been treated as wideband plane waves and their approximate directions of arrival (DOA) are estimated by using two different methods. The usefulness (besides the apparent one) of the results of the DOA estimation in the problem of estimating the coherence of the array (vertical or tilted positioning) is discussed. Finally the array gain, based on the experimental data, is computed and compared with the theoretical, as another important measure of array performance. It is seen that the difference of these two is always less than 3 dB. The noise field along with its vertical directivity are proven to be decisive factors in the above computation, and therefore, in the assessment of the array's performance.

intentionally blank page

Performance assessment of the SACLANTCEN vertical array in shallow water

A. Bassias

Abstract: In this memorandum the performance of the SACLANTCEN vertical array is assessed, based on an analysis of experimental data collected in shallow water during the October–November 1991 Signal Processing Group sea trial. The measures that have been used for the assessment of the performance of the vertical array, as well as for the evaluation of the quality of the data, for both the signal and noise fields, seen from both signal processing and statistical points of view, constitute a method that leads to the conclusion whether the array performed as expected. These measures are a survey of the sensors' outputs in the time-domain, computation of spectra both for the signal (plus noise) and purely noise parts, computation of the auto-correlation functions for the sensors' outputs as well as the cross-correlation functions between outputs of selected sensors, and computation of histograms from both signal and noise samples. Furthermore, by treating the received signals at the array – which were test signals – as wideband plane waves, their approximate directions of arrival (DOA) are estimated by using two different methods. The first method is the classical broadband beamforming algorithm and the second method is the coherent signal-subspace (CSS) method, both in the frequency domain. The usefulness (besides the apparent one) of the results of the DOA estimation in the problem of estimating the coherence of the array (vertical or tilted positioning) is discussed. Finally the array gain, based on the experimental data, is computed and compared with the theoretical one as another important measure which is an indicator that the array would be fit for its intended use. The noise field along with its vertical directivity are proven to be decisive factors in the above computation, and therefore in the assessment of the array's performance.

Keywords: array gain ○ beamforming ○ coherent signal subspace (CSS) ○ fast fourier transform (FFT) ○ performance assessment ○ vertical array

Contents

1 Introduction

This memorandum provides an assessment of the performance of the SACLANTCEN vertical array based on an analysis of experimental data collected in shallow water during the October–November 1991 Signal Processing Group sea trials. The methods which were used to assess the performance of the vertical array are enumerated, their theoretical foundation is provided and results from their use with experimental data are presented.

The measures used both for the assessment of the performance of the vertical array, and for the evaluation of the quality of the data, for both the signal and noise fields, constitute a methodology for ascertaining whether or not the array performed as expected. From a review of the literature on the evaluation of data and on the assessment of a vertical array, both theoretically and experimentally (Anderson, 1979; Buckingham and Jones, 1987; Hamson, 1979, 1980; Hodgkiss and Fisher, 1990; Hollett, 1992; Sotirin and Hodgkiss, 1989; Tyce, 1982), or assessing the performance of a towed array, in real-time, (Wagstaff et al., 1982), it may be concluded that the proposed measures are suitable for the vertical array.

The signals received at the array are treated as wideband plane waves, therefore, the beamforming algorithm, which is primarily used for the detection of the received signals and the estimation of their angle of arrival, is the classical broadband beamforming algorithm in the frequency domain. The assumption of plane waves for the signals is valid and provides a fairly good approximation because, due to the distance between the acoustic source and the vertical array, the curvature of the wavefronts is considerably reduced (Clay and Medwin, 1977). The beamformer is used to estimate the approximate direction of arrival (DOA) of the signals and involves decomposition of the received signals in the frequency domain, using FFT (fast Fourier transform) at the individual hydrophone outputs and then averaging of the beamformer's outputs over the individual temporal frequencies. The term temporal frequency will be used in contrast to the term spatial frequency, which is directly associated with the angles of arrival. A model formulation with the basic assumptions about the signals, the noise and the beamforming algorithm along with the equations involved, will be given in the following. For the sake of comparison and for higher resolution, a second direction of arrival technique, the coherent signal-subspace (CSS) method (Wang and Kaveh, 1985) will be used. The processing of experimental wideband signals for the estimation of their angle of arrival by using the CSS method is introduced for the first time at SACLANTCEN. Also in the literature there are no reported results on the performance of the CSS method with experimental data collected by a vertical array. The CSS method is also based on the decomposition of

the signals in the frequency domain but, in addition, performs coherent averaging of transformed spatial covariance matrices at individual temporal frequencies. The CSS is a preprocessing method and at its final stage it makes use of any high resolution eigen-decomposition based method for narrowband signals such as MUSIC (multiple signal classification) (Schmidt, 1978) or minimum norm (Kumaresan and Tufts, 1983), in order to estimate the angle of arrival of signals received by an array. Since the CSS method along with the MUSIC and minimum norm algorithms, as its final stage, were used in the processing of the data, a brief presentation of these algorithms will be given, followed by a brief presentation of the CSS method. The results of the processing of the data, in which all the above-mentioned methods were used, is then given.

The structure of this memorandum is as follows. First, there is a description of the experiment and the data collected. Next, a number of measures and the results of the application of these measures to experimental data, are described. These measures are a survey of the hydrophones' outputs, computation of spectra, autocorrelation and cross-correlation functions of the hydrophone outputs, computation of histograms and statistics of the received signals at the hydrophones. Next, a general model is developed for the received signals and, based on this model, the classical beamforming algorithm and the MUSIC, minimum norm and CSS algorithms are described. Following the results in which these methods were used, the problem of estimating the coherence of the array (vertical or tilted), is discussed. The array gain, signal gain and noise gain are defined and details of the way in which they were used with the experimental data, are given. Note here that the term 'signal' means, of course, signal plus noise, while the term 'noise' denotes noisy samples only. However, for simplicity the terms signal and noise will be used correspondingly throughout this memorandum. A short theoretical analysis of the low-frequency part of the array (i.e. the 32 hydrophones spaced 2 m apart) is given separately in Appendix A. For each measure, The purpose, usefulness and limitations of all the measurements are given, and it is also explained how they demonstrate that the array was operating as expected.

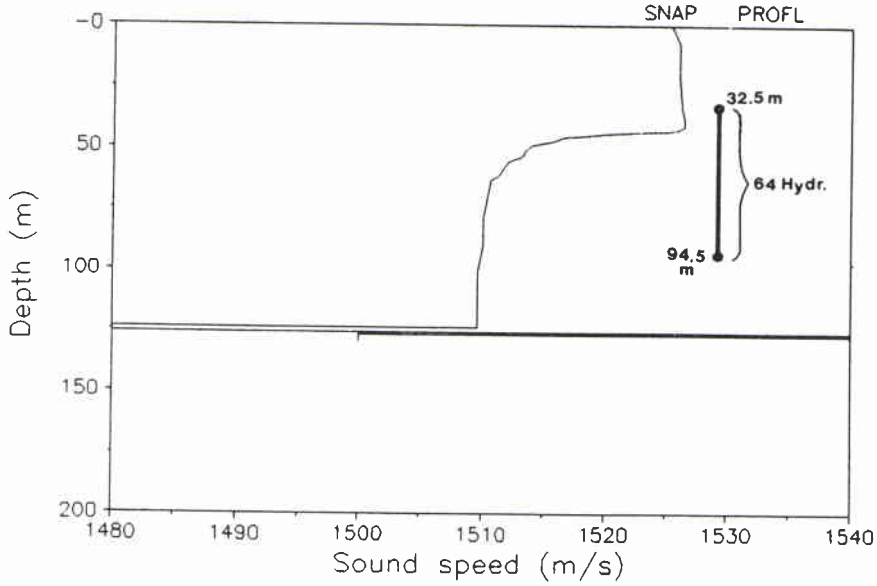

Figure 1 *Sound-velocity profile and array position during the experiment.*

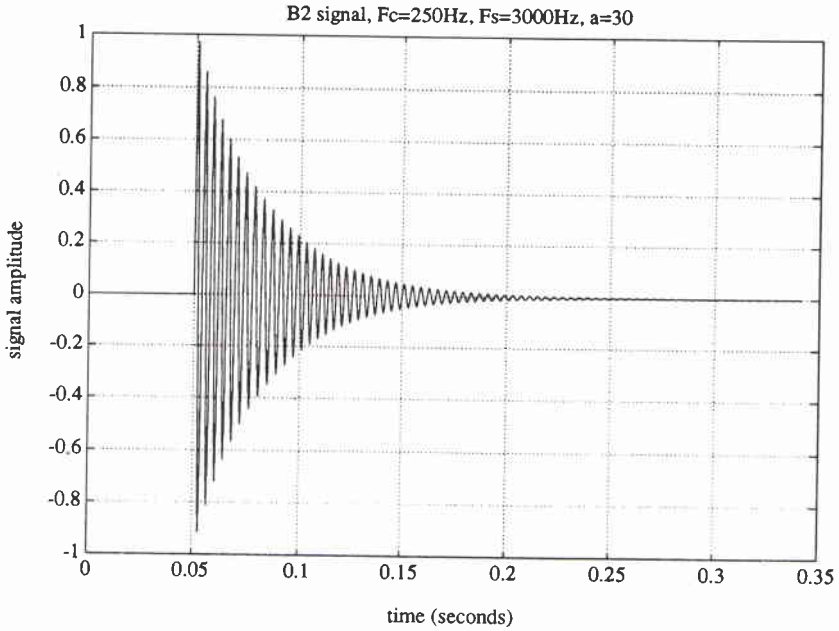

Figure 2 *B2 coded signal (damped sinusoid).*

1.1. EXPERIMENTAL INFORMATION

The performance assessment is based on data collected in shallow water (124 m depth, approximately). The area of this trial was in the Mediterranean Sea. The array was bottom moored and the first hydrophone (channel 1) was located at 32.5 m depth while the 64th hydrophone (channel 64) was at 94.5 m. The position of the array and the sound-velocity profile is shown in Fig. 1. The set of data that was used was collected during an experiment of 10 min duration, approximately. A stationary, omnidirectional acoustic source was located at 60 m depth and at a 4 km range from the array. During the experiment the source transmitted every 5 s an exponentially damped sinusoid centred at a carrier frequency $f_c = 250$ Hz and has a duration of 0.1 s, bandwidth $B = 9$ Hz, time delay $t_0 = 50$ ms and a damping coefficient $a = 30$. Mathematically this signal is described by the following formula:

$$s(t) = \sin(2\pi f_c(t - t_0)) \exp[-\alpha(t - t_0)]u(t - t_0), \tag{1}$$

where $u(t)$ is the step function. The above signal was sampled in time at a sampling frequency $f_s = 3000$ samples/s and is shown in Fig. 2. The data received by the array were subjected to onboard processing such that the repetition rate of the existing retrieved pings is changed to 2.048 s, i.e. one ping every 2.048 s (duration of each ping is 2.048 s), and a spectral content which is limited, essentially, to a band from 225 to 275 Hz as will be seen in the next section. The exact number of available pings is 149 and covers 305.152 s of data.

2 Performance assessment

For each measure, a large number of data were studied, but here only samples of the results will be shown since the rest of them are similar and their presentation would add nothing to the conclusions. The following measures were used in order to assess the performance of the vertical array during the experiment.

Measure 1 The sensors' outputs in the time domain were surveyed for the verification of the functioning of the sensors. The outputs may be broadly separated into two groups. A group in which the presence of signal amidst noise is obvious and a group in which the absence of a signal, or the presence of noise only, is obvious. In this particular experiment the task of identifying the signal is not difficult, since the signal was quite strong on all sensors and easily distinguishable from background noise, as may be seen in the figures. For the second group, as noise were considered to be samples, in time, far from the beginning of each ping (1.3 s approximately) or, in other words, samples just before start of the the next ping. For this selection we used our judgement and it should be noted that there may be more than one way to do this. Figure 3(a) shows 0.68 s from the first ping as it was received by all 64 hydrophones. This shows that all hydrophones were functioning and receiving. The rest of the figures will show the output of the low-frequency part of the array only, i.e. outputs from the 32 hydrophones spaced at 2 m apart. So, Fig. 3(b) shows the separate outputs of these hydrophones for the second ping. The presence of signal is obvious in these figures. In the case of noise, and because of its lower amplitude which makes it more difficult to see in this kind of figure, other type of graphics are used. Figure 4 shows hydrophone outputs during the noise prevailing part of ping1. Note that the amplitudes of the signals are relative and do not correspond to any actual physical units. The signals look slightly rounded but this is due to the fact that the hydrophone outputs were filtered and their spectrum is essentially confined in a narrow band. The filtering has also resulted in a signal-like noise, a fact that will be verified in subsequent sections where auto-correlation and cross-correlation of the data are examined and beamforming is performed.

Measure 2 Spectra were computed both for the signal and noise parts, i.e. using samples that the previous step has shown contain information about the signal and, for the noise part, samples that do not contain such information. The spectra were obtained using DFTs (discrete Fourier transforms) as follows. Let $\mathbf{x}_n \equiv [x_n(1), \ldots, x_n(K)]^{\mathrm{T}}$ be the vector of K samples of the nth hydrophone output. So, we have an array $\mathbf{X} \equiv [x_1, \ldots, x_N]$ of these vectors, where N is the number of hydrophones. Note that throughout this study, lowercase boldface letters will indicate vectors while uppercase boldface letters will indicate matrices. By performing

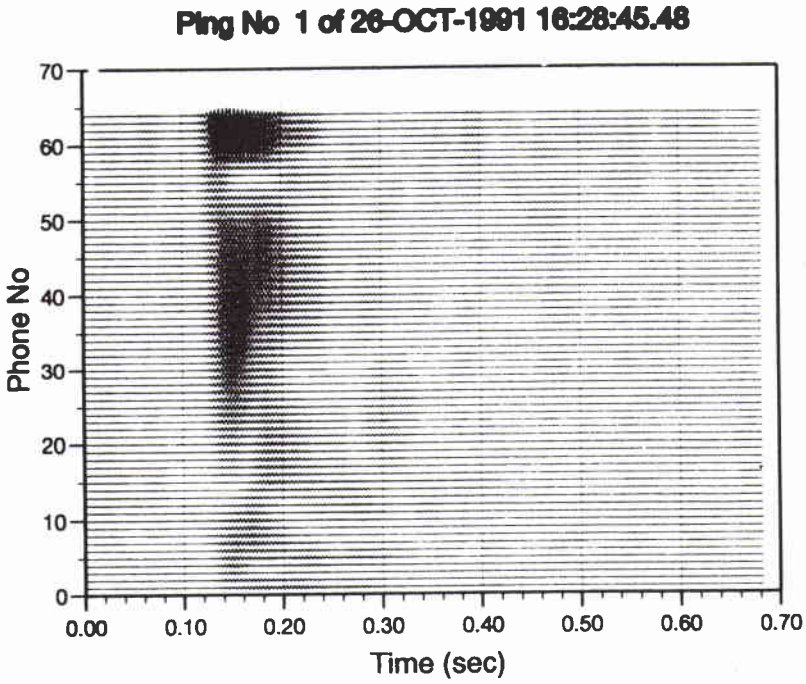

Figure 3(a) *Example of the output of the 64 hydrophones in the time domain with experimental data. The number of samples is 2048.*

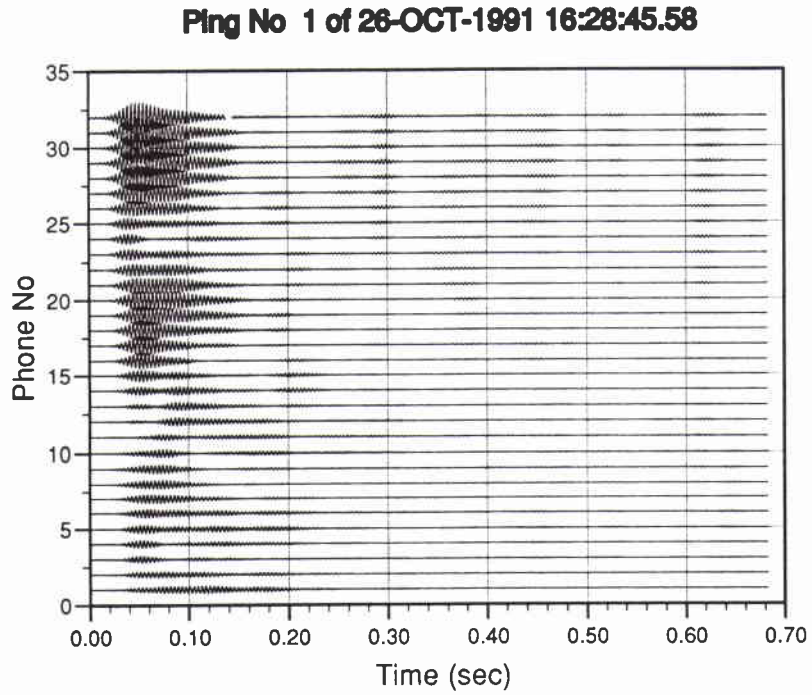

Figure 3(b) *Example of the output of the 32 hydrophones (low frequency part of the array) in the time domain with experimental data. The number of samples is 2048.*

DFT on the output of the nth sensor we obtain the jth element of the vector $\mathbf{x}_n$ in the jth frequency f_j, i.e. (Oppenheim and Schafer, 1975)

$$x_n(f_j) = \sum_{k=1}^{K} x_n(k) e^{-i2\pi f_j k/K}, \tag{2}$$

where $i = \sqrt{-1}$. The spectral power of the nth hydrophone output at the jth frequency is given by

$$X_n(f_j) = 10 \log |x_n(f_j)|^2. \tag{3}$$

The information obtained from this step is very useful because it verifies the existence of signal and the spectral differences between signal and noise parts. For the case of signal spectrum, due to the short signal duration, a number of $N = 512$ samples was judged to be adequate for the computation of the spectra which may be seen, for various hydrophone outputs during the first ping, in Fig. 5. In the case of noise the spectra for various pings are shown in Fig. 6. In both cases the spectra are centred close to or on 250 Hz and, also due to onboard processing, are confined to a rather narrow band covering frequencies essentially from 225 to 275 Hz. The noise spectra present a more intense flatness and fluctuation, as expected. The knowledge of the spectra was used in the beamforming as well as for the computation of the signal and noise gains. It also provides valuable insight in the noise structure and helps to interpret other measures, such as the kind of noise that was present during the experiment.

Measure 3 The auto-correlation functions for the sensors' outputs as well as the cross-correlation functions between outputs of selected sensors were computed as follows. The auto-correlation function $C_{x_n x_n}(m)$ of the nth hydrophone output sample vector at the mth moment is defined by means of the expected value of $x_n(k)$, $k = 1, \ldots, K$ as

$$C_{x_n x_n}(m) = E[x_n(k) x_n^*(k+m)], \tag{4}$$

and its unbiased estimate is computed by (Bendat and Piersol, 1971),

$$C_{x_n x_n}(m) = \frac{1}{K - |m|} \sum_{k=1}^{K-|m|} x_n(k) x_n^*(k+m), \tag{5}$$

where '*' indicates the conjugate of a complex number. The cross-correlation function $C_{x_n x_l}(m)$ at the mth moment between two different output sample vectors x_n and x_l is defined as

$$C_{x_n x_l}(m) = E[x_n(k) x_l^*(k+m)], \tag{6}$$

and its unbiased estimate is computed by

$$C_{x_n x_l}(m) = \frac{1}{K - |m|} \sum_{k=1}^{K-|m|} x_n(k) x_l^*(k+m). \tag{7}$$

The computation of these functions provides information about the resemblance of the received signals to themselves, in the case of auto-correlation, and between outputs of adjacent hydrophones as well as between outputs of distant hydrophones, in the case of cross-correlation.

Figure 7 show the auto-correlation, during the first ping, of the outputs of some of the 32 hydrophones which comprise the low frequency part of the array. For these figures 1000 samples were used. It can be seen that the values vary from almost zero, for samples of noise, to 1 for samples of only signal. The auto-correlation of the noise part of ping1 is shown in Fig. 8. Contrary to what is expected for noise, this noise has a high degree of self similarity. Figure 9 shows the correlation between outputs of different hydrophones. The degree of similarity among them is clearly seen in these cases, as can also be seen, but in a lesser degree, in Fig. 10 where the correlations between noise only containing outputs of various hydrophones, during ping1, are shown. Figure 11 shows how the noise only containing outputs of certain hydrophones during different pings are correlated. As expected, the degree of similarity is lower in these cases. Finally, Fig. 12 shows the correlation between signal and noise in various hydrophones for data samples selected from the same ping. It can be seen that there exists a degree of similarity even between signal and noise parts but it is not high. From all the previous figures it may be concluded that the noise is slightly correlated with both itself and with the signals.

Measure 4 Histograms were computed for both signal and noise samples from the various hydrophone outputs and a sample of the results is shown in the next two figures. Due to the short duration of the transmitted signal the number of samples that was used was 500. Note that the horizontal axis in these figures is automatically scaled thus, the range is different from figure to figure. Figure 13 shows the histograms for signal samples selected from the outputs of some of the 32 hydrophones during ping1, while Fig. 14 shows the histogram of 500 noise samples selected from the outputs of the same hydrophones as before. The difference in the statistics between signal and noise can be seen, but from the noise histograms it cannot be concluded that the noise has any of the known statistics, in spite the fact that for some hydrophone outputs, the histograms suggest that the noise is close to being Gaussian. In all cases, both the signal and noise are zero mean stochastic processes and their standard deviation varies from hydrophone to hydrophone, a fact which can be easily appreciated by observing the amplitudes of the individual hydrophones. In the following sections the received signals are treated as wideband plane waves. A model for these plane waves is formulated in the development of the broadband, classical beamforming algorithm as well as for the MUSIC, minimum norm-based CSS algorithm in the frequency domain. The advantages and the limitations of each of the above algorithms, of course are mentioned. Then the array gain, signal gain and noise gain are defined and analytical mathematical expressions are given in order to compute them in the frequency domain.

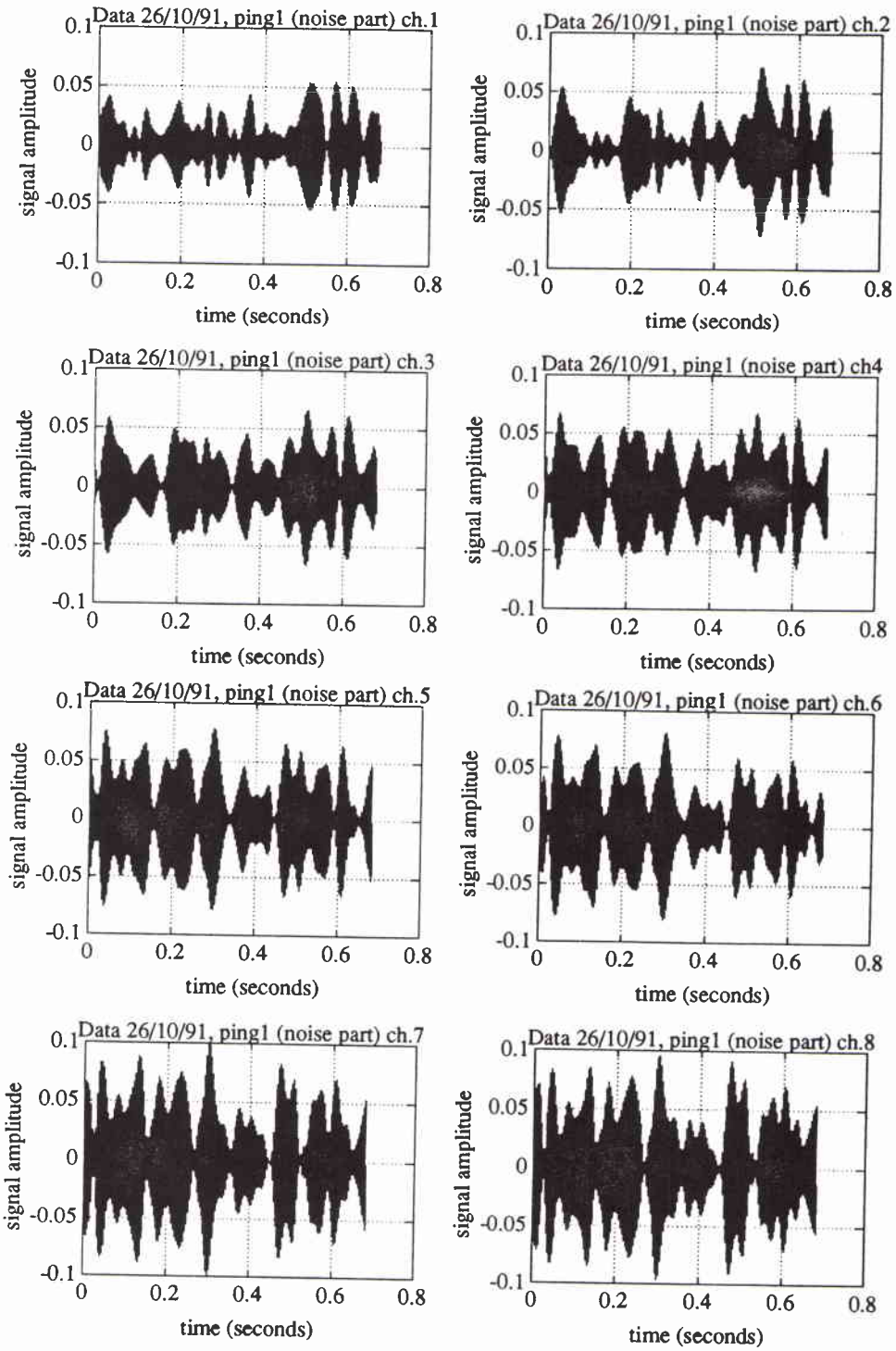

Figure 4 *Hydrophone outputs during the noise prevailing part of ping1.*

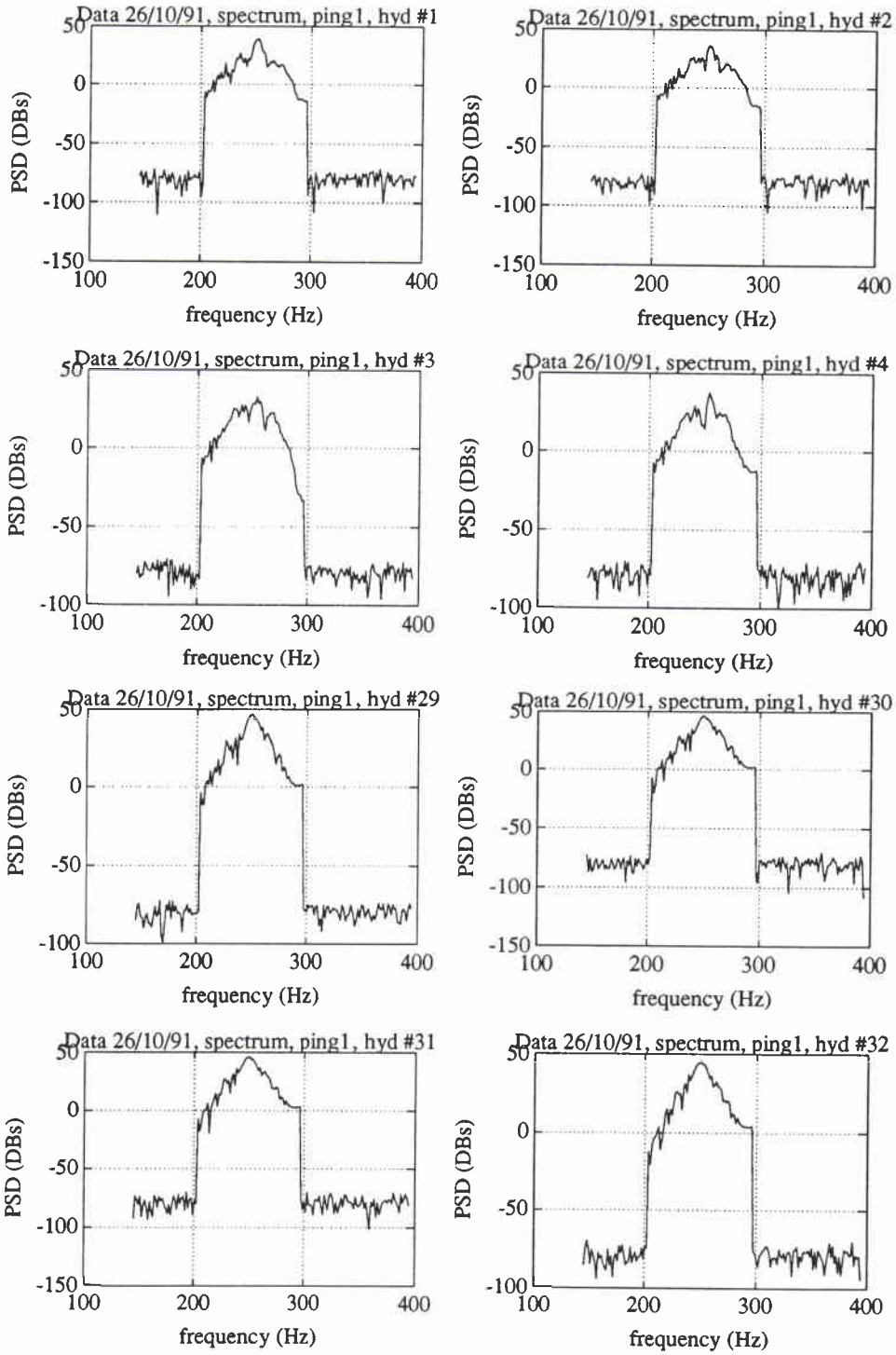

Figure 5 *Spectra of some of the hydrophone outputs containing only the signal part of various pings.*

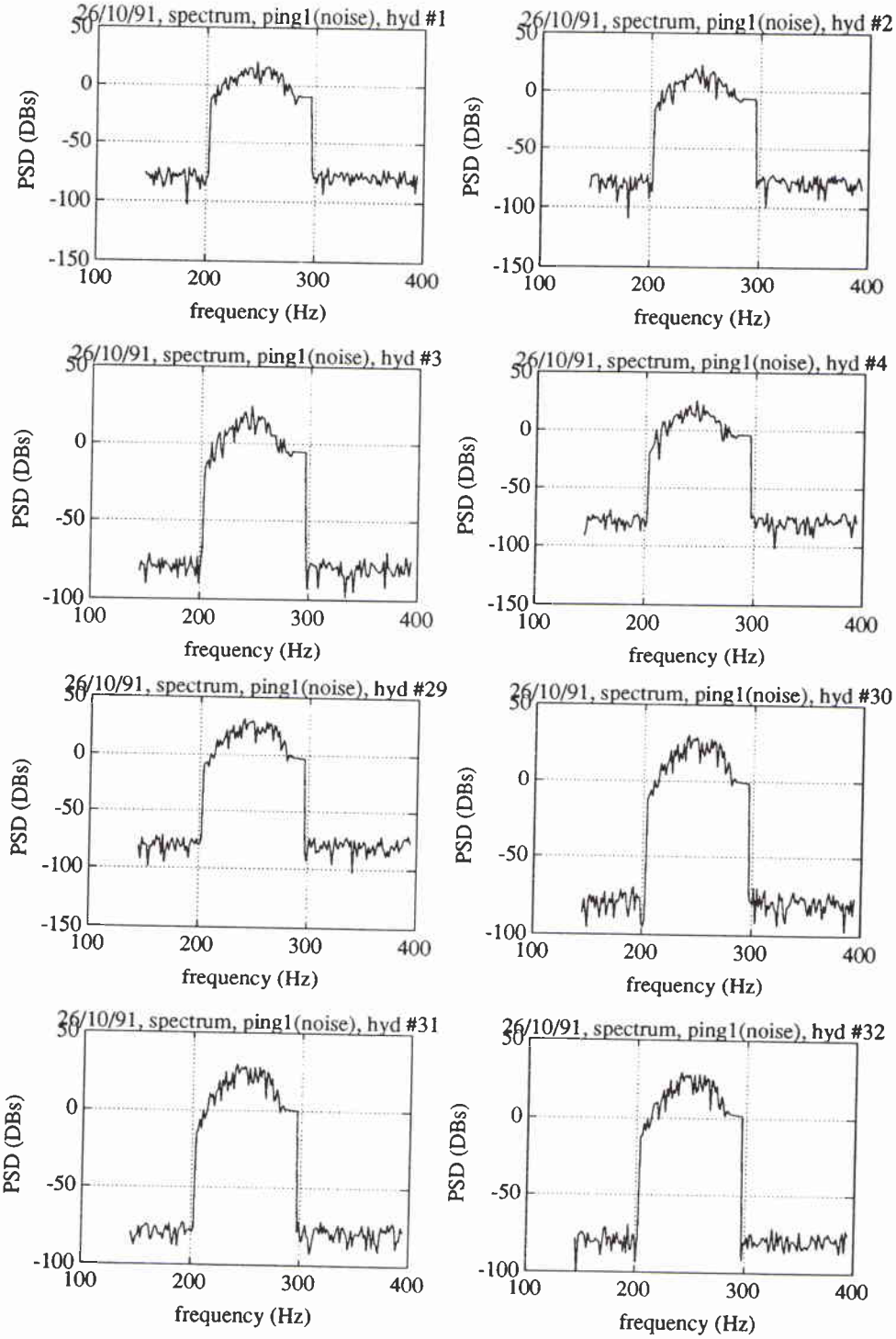

Figure 6 *Spectra of some of the hydrophone outputs containing only the noise part of various pings.*

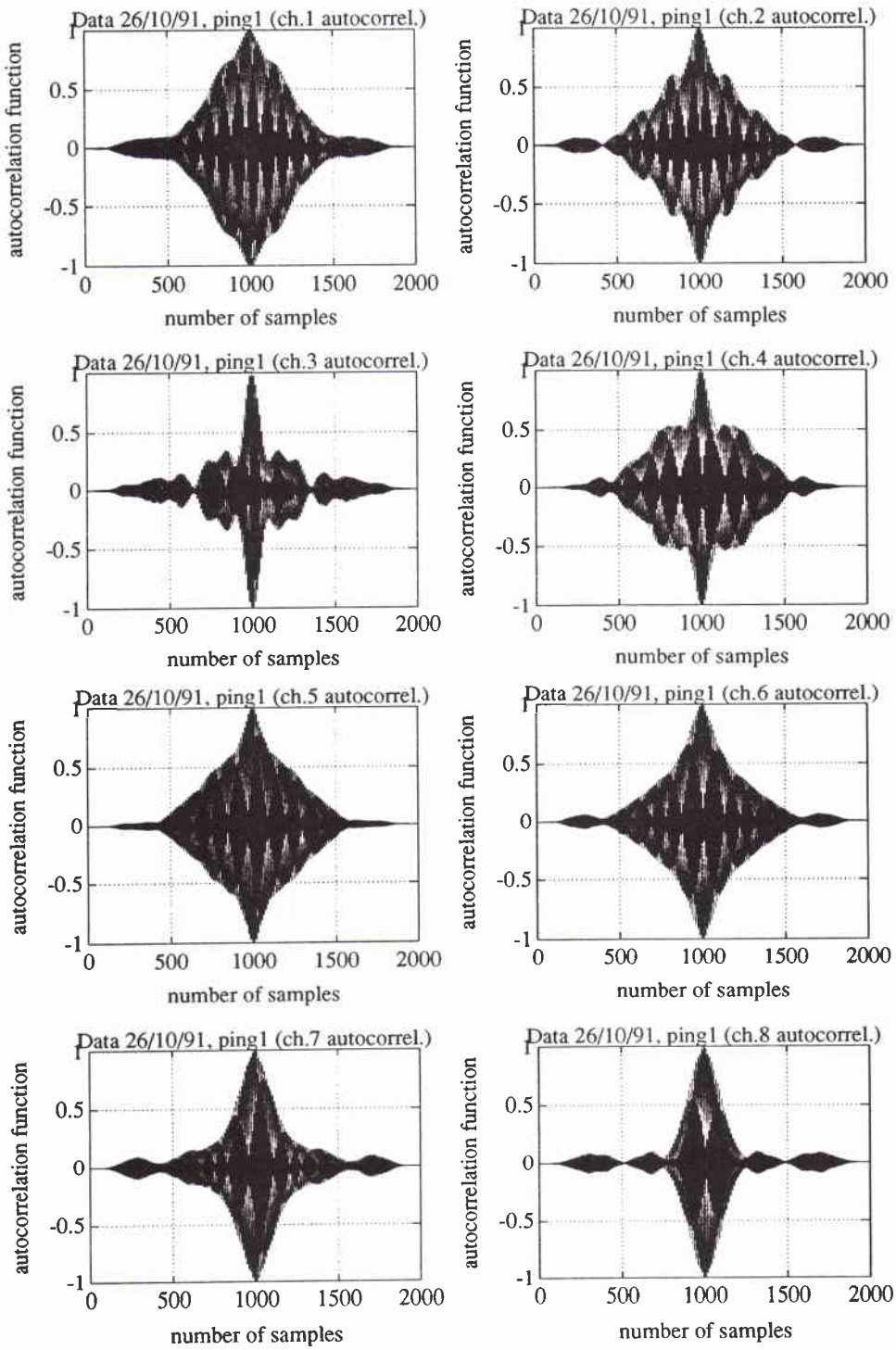

Figure 7 *Auto-correlation of some of the 32 hydrophone outputs during the signal prevailing part of ping1.*

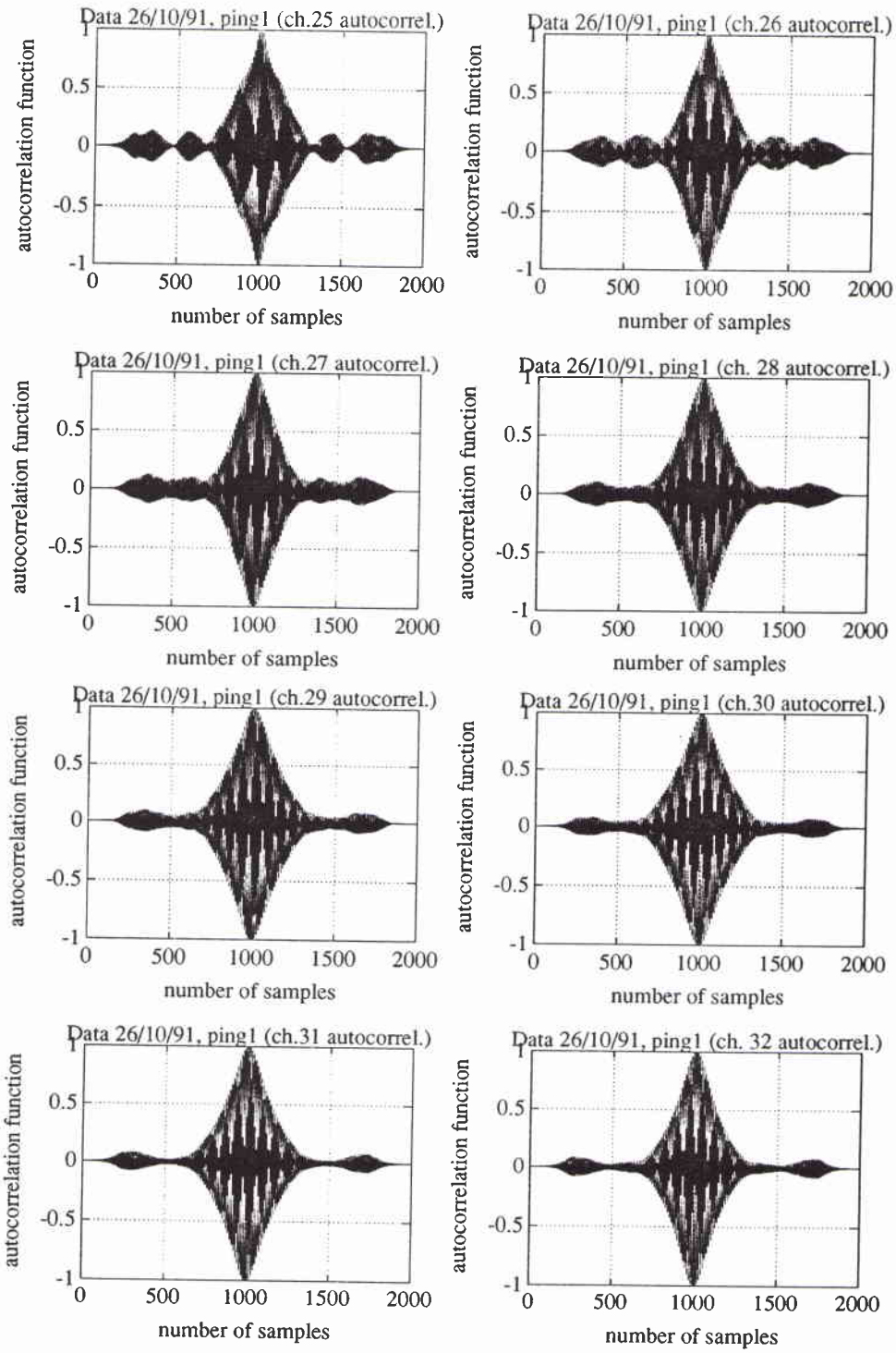

Figure 7 (cont'd) *Auto-correlation of some of the 32 hydrophone outputs during the signal prevailing part of ping1.*

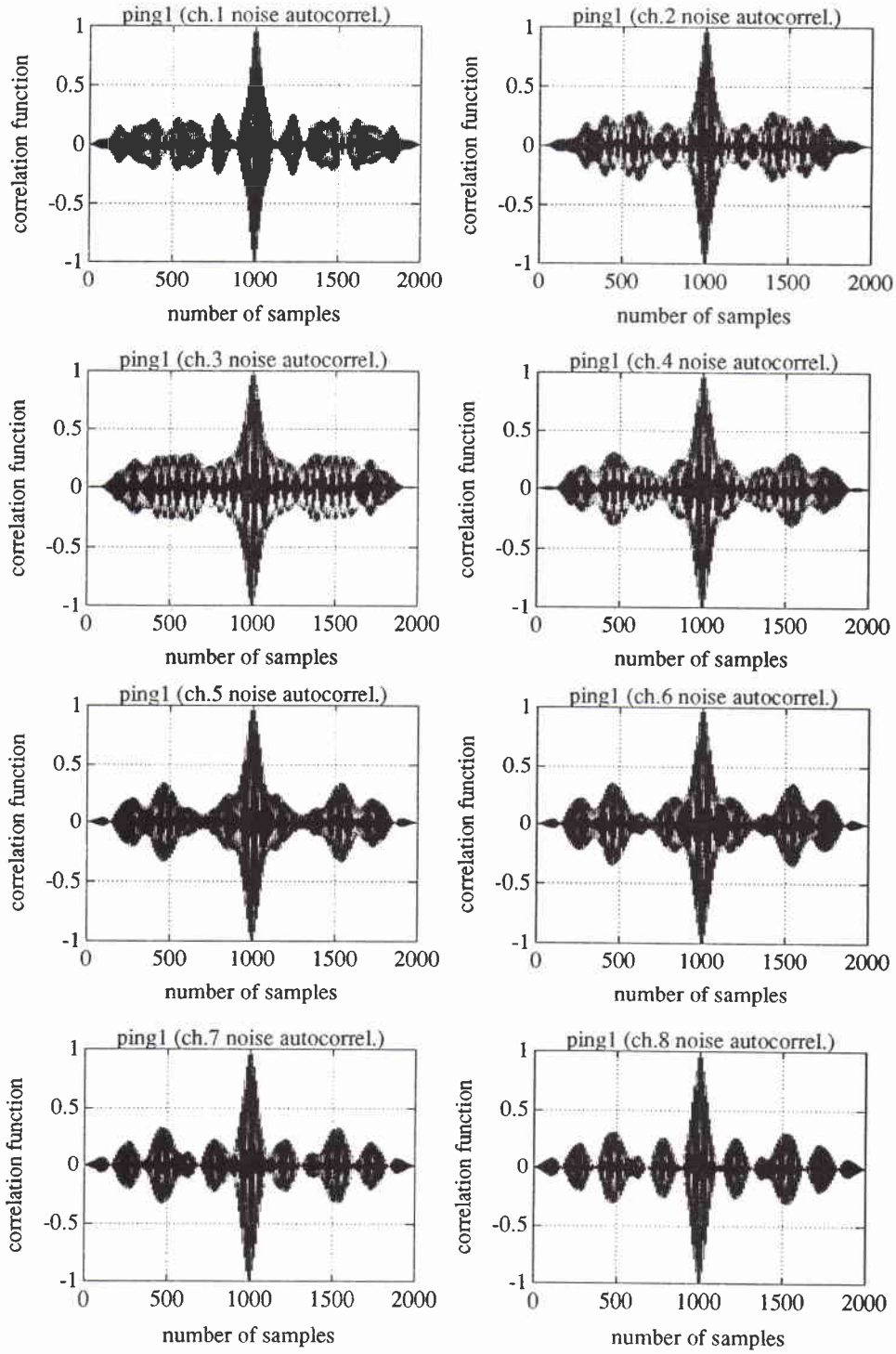

Figure 8 *Auto-correlation of some of the 32 hydrophone outputs during the noise prevailing part of ping1.*

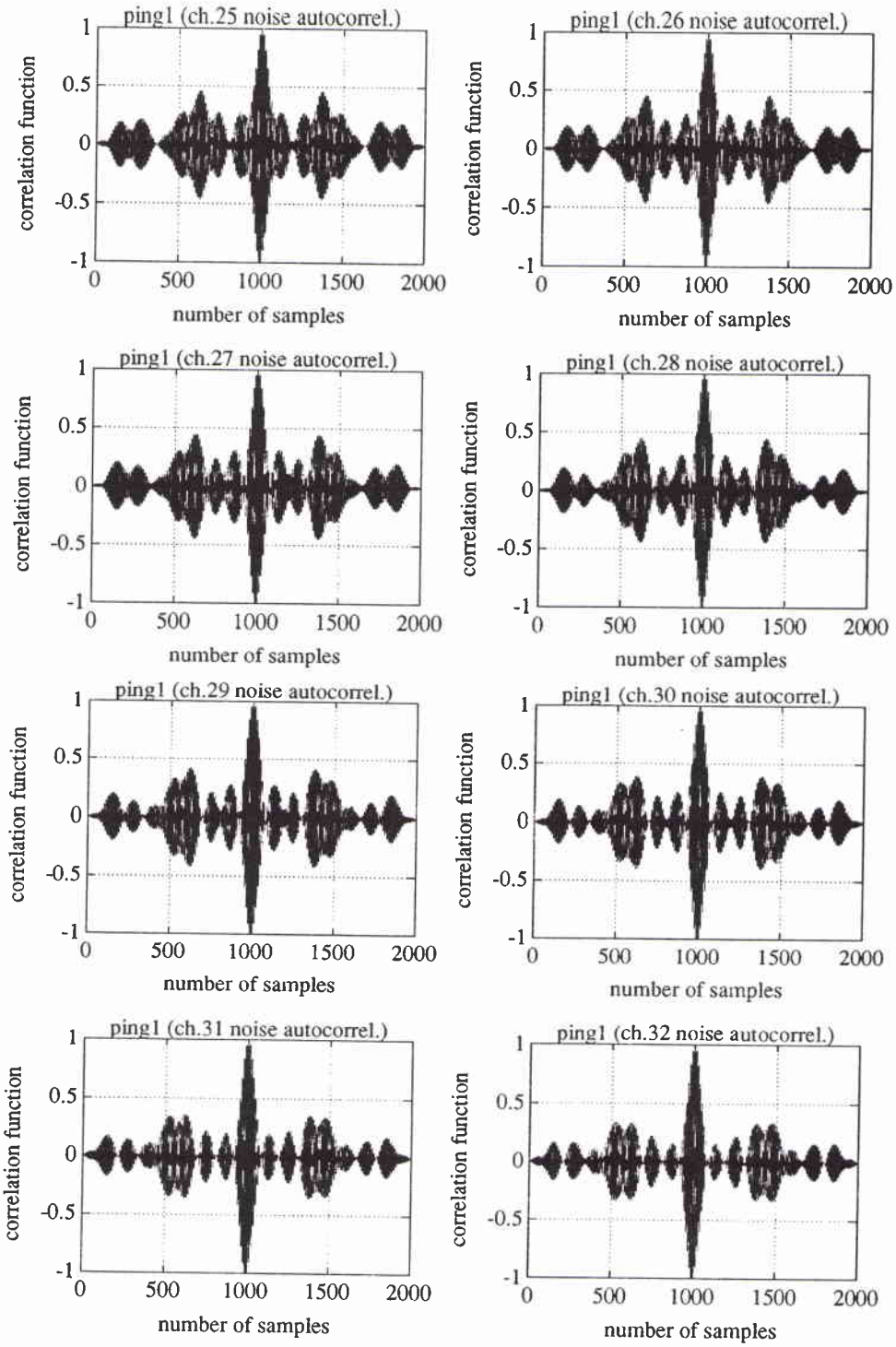

Figure 8 (cont'd) *Auto-correlation of some of the 32 hydrophone outputs during the noise prevailing part of ping1.*

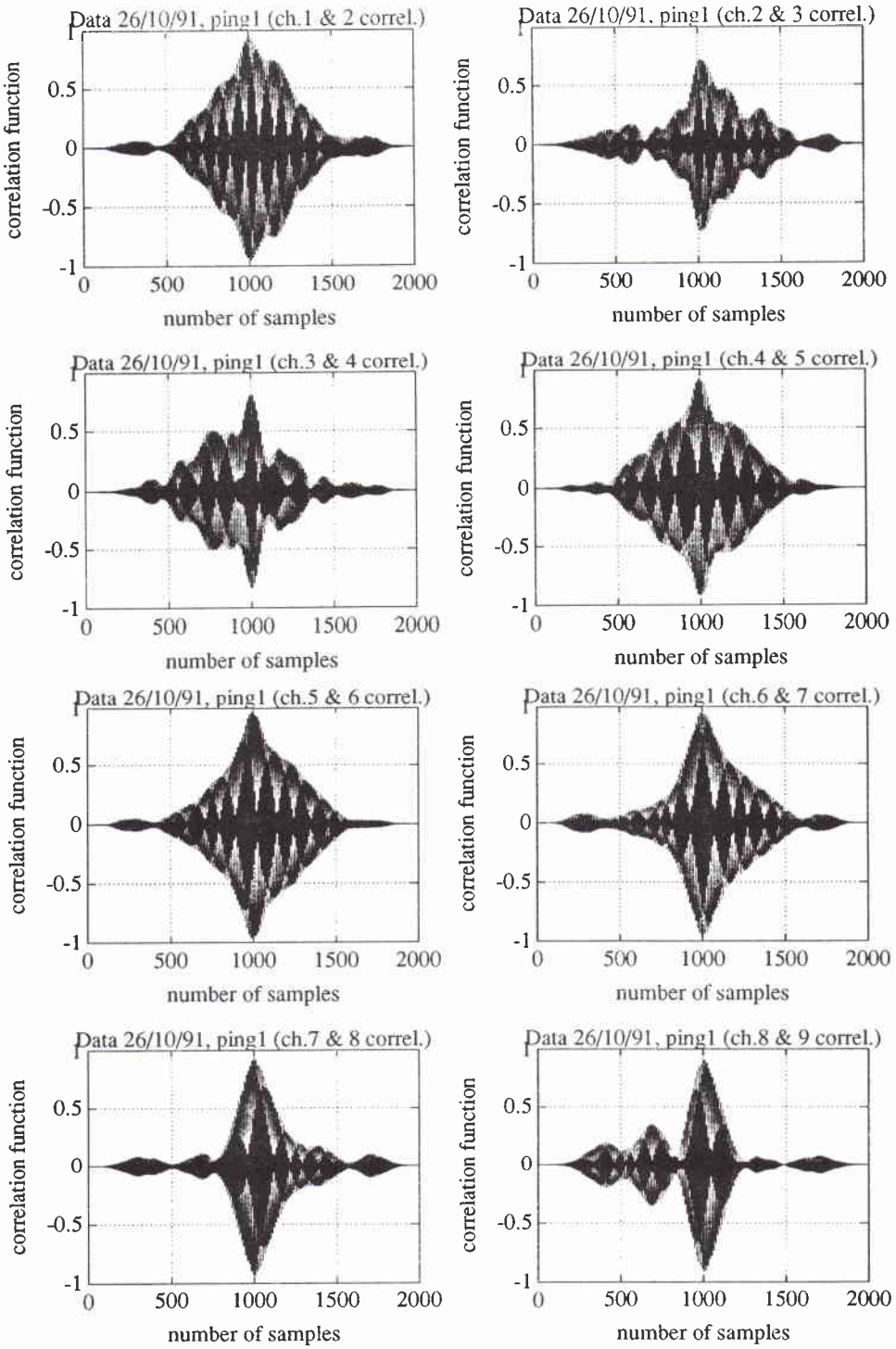

Figure 9 *Cross-correlation between outputs of different hydrophones during the signal prevailing part of ping1.*

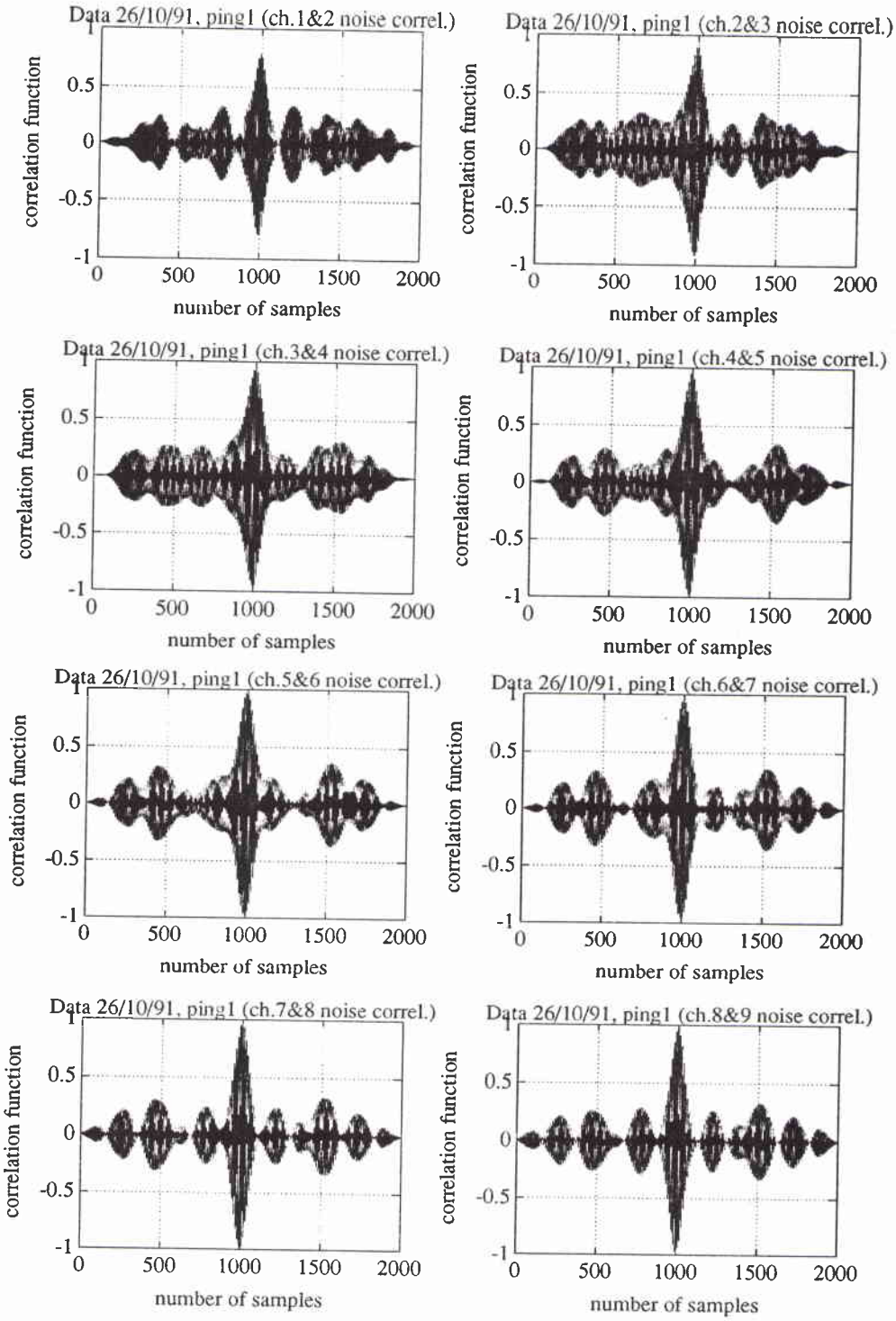

Figure 10 *Cross-correlation between outputs of different hydrophones during the noise prevailing part of ping1.*

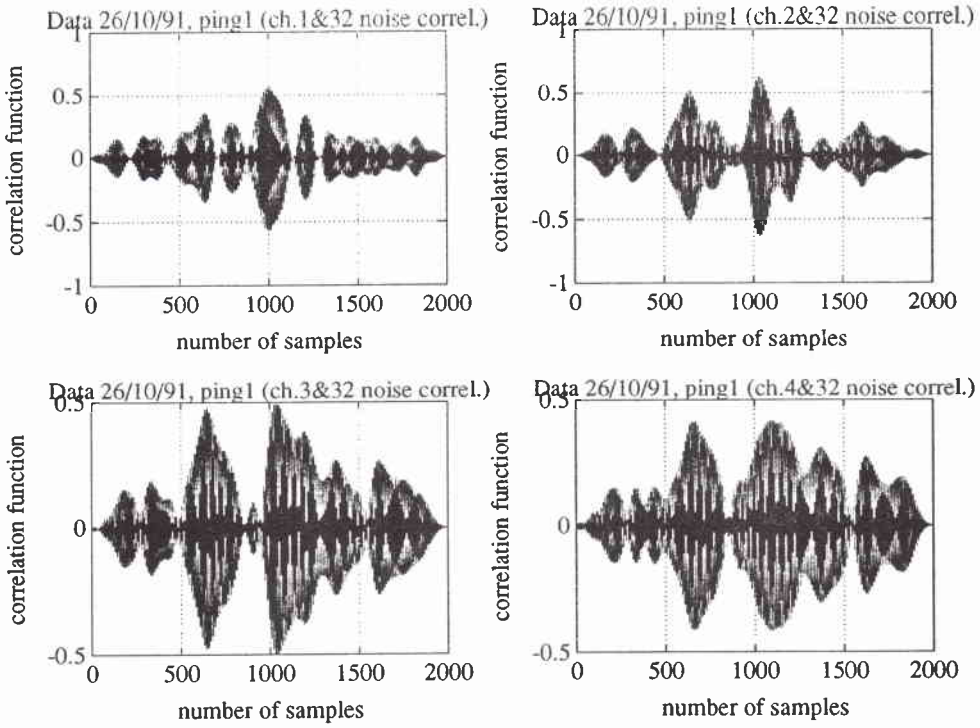

Figure 10 (cont'd) *Cross-correlation between outputs of different hydrophones during the noise prevailing part of ping1.*

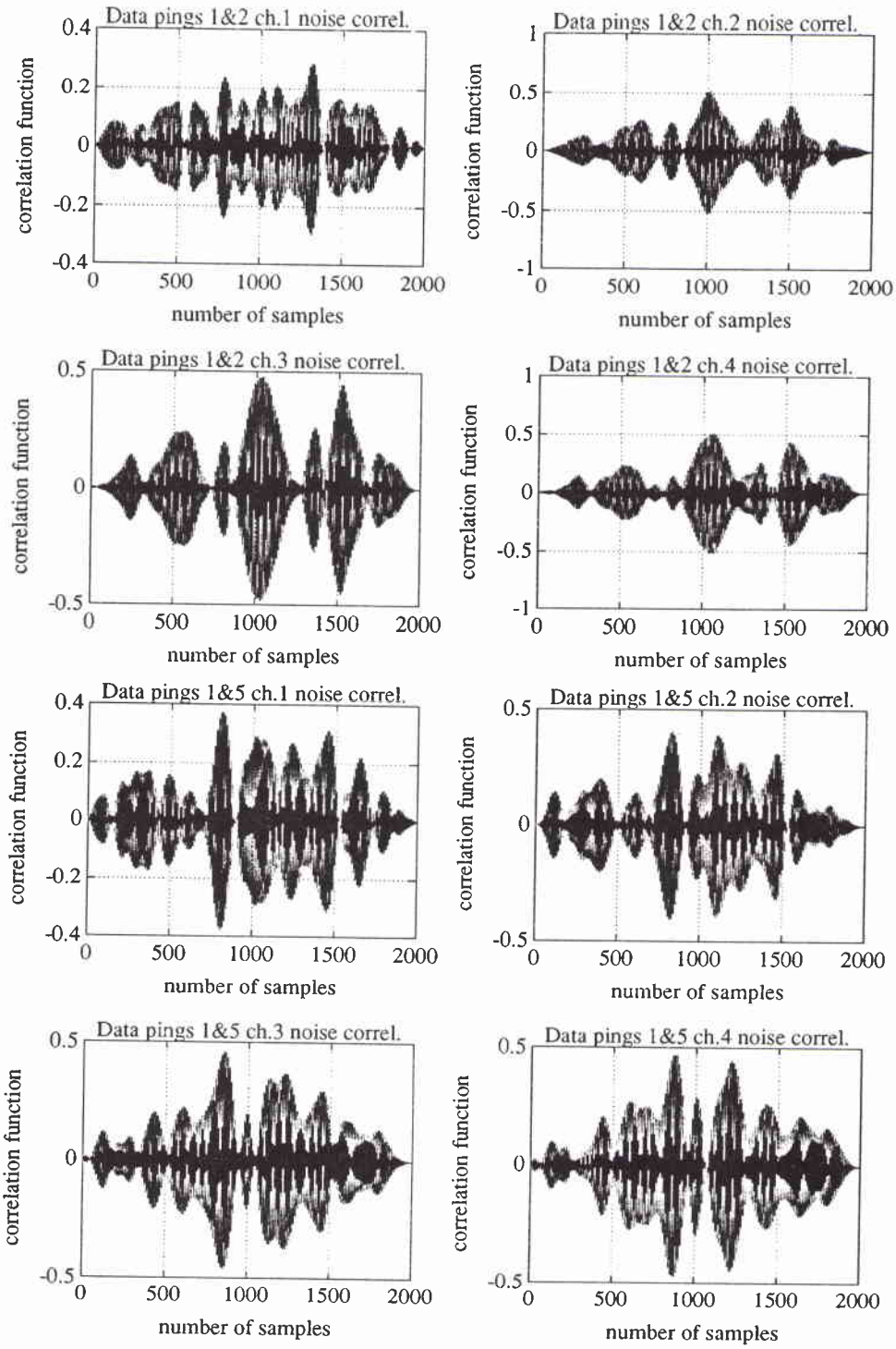

Figure 11 *Cross-correlation between outputs of certain hydrophones during the noise prevailing part of different pings.*

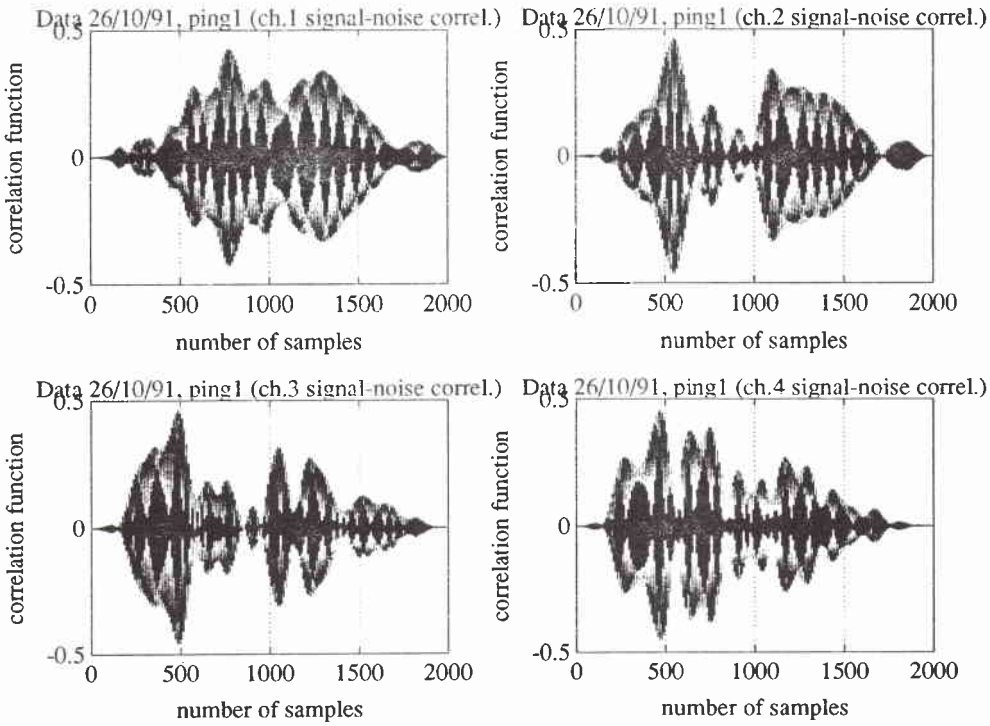

Figure 12 *Cross-correlation between signal and noise parts of various hydrophone outputs during the same ping.*

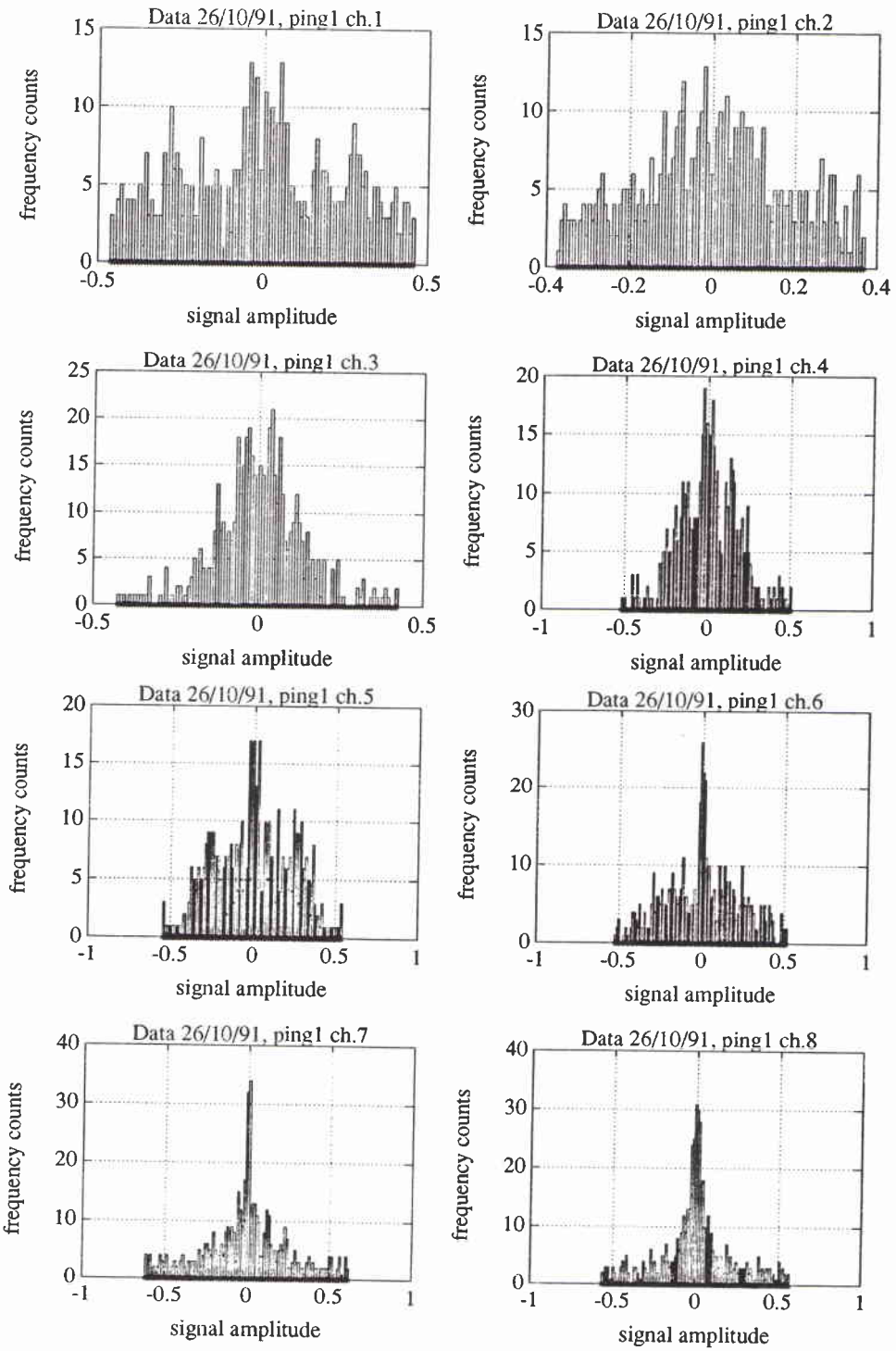

Figure 13 *Histograms of samples selected from the signal prevailing part of some of the outputs of 32 hydrophones during ping1.*

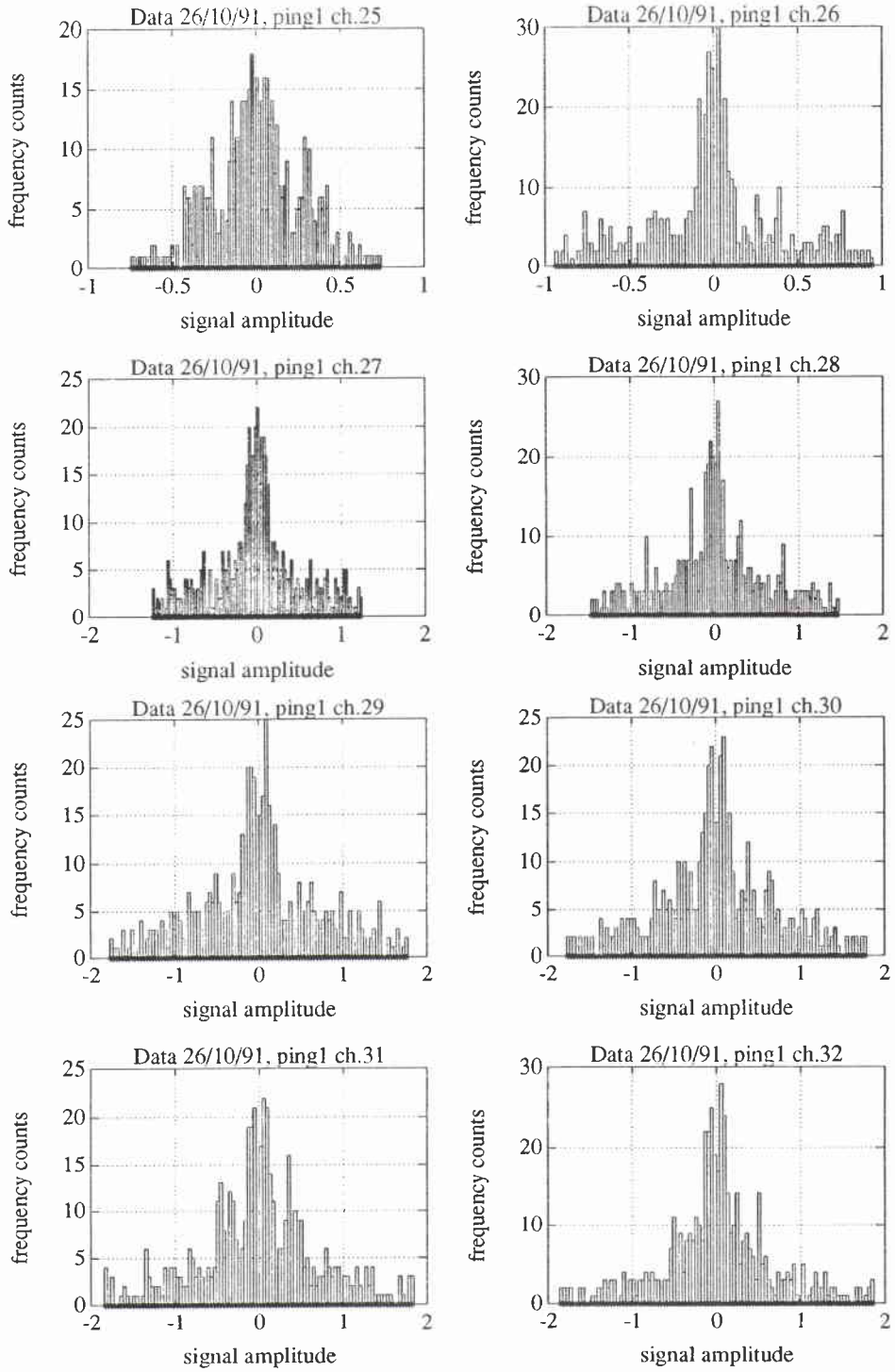

Figure 13 (cont'd) *Histograms of samples selected from the signal prevailing part of some of the outputs of 32 hydrophones during ping1.*

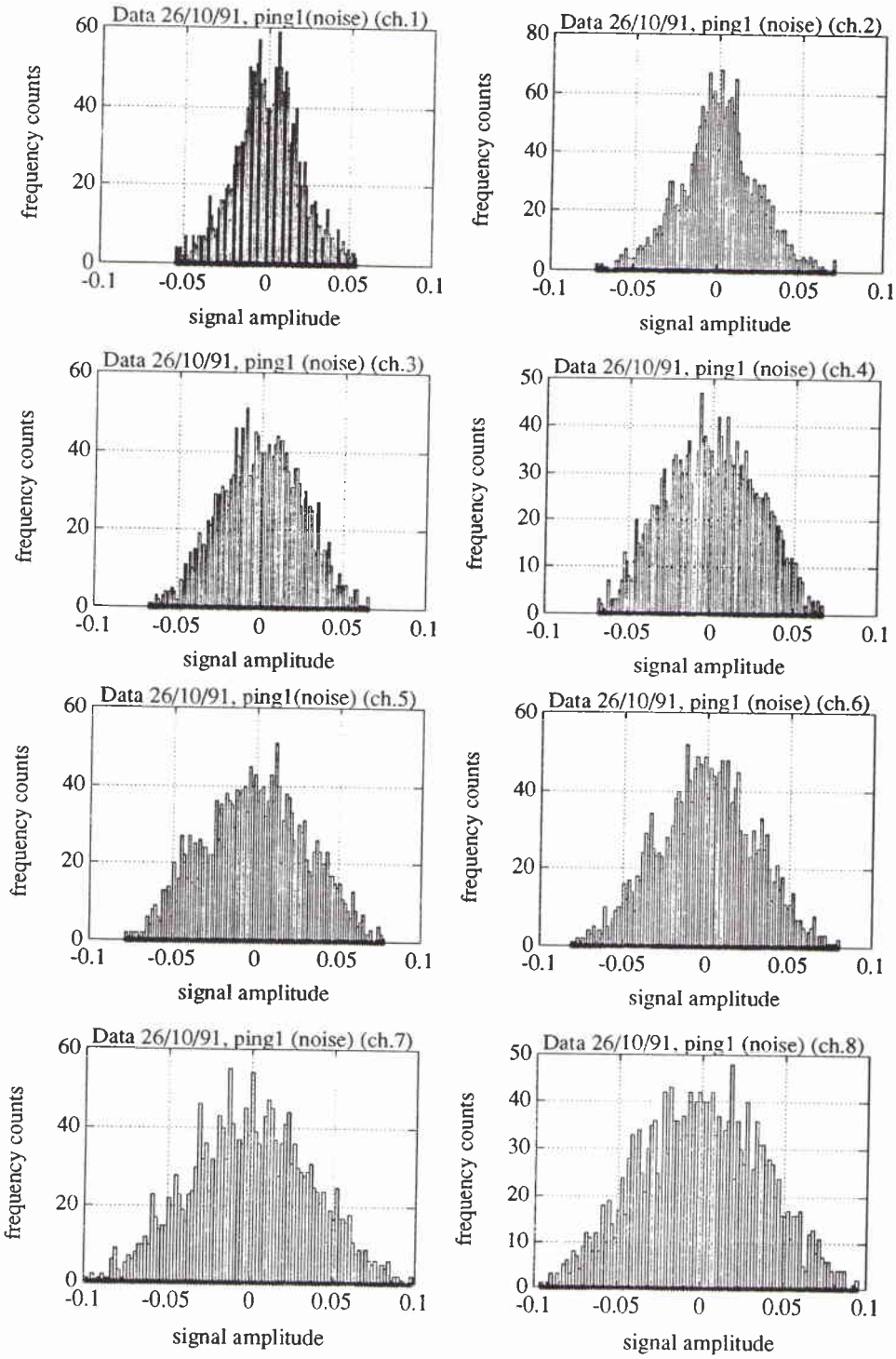

Figure 14 *Histograms of samples selected from the noise prevailing part of the outputs of 32 hydrophones during ping1.*

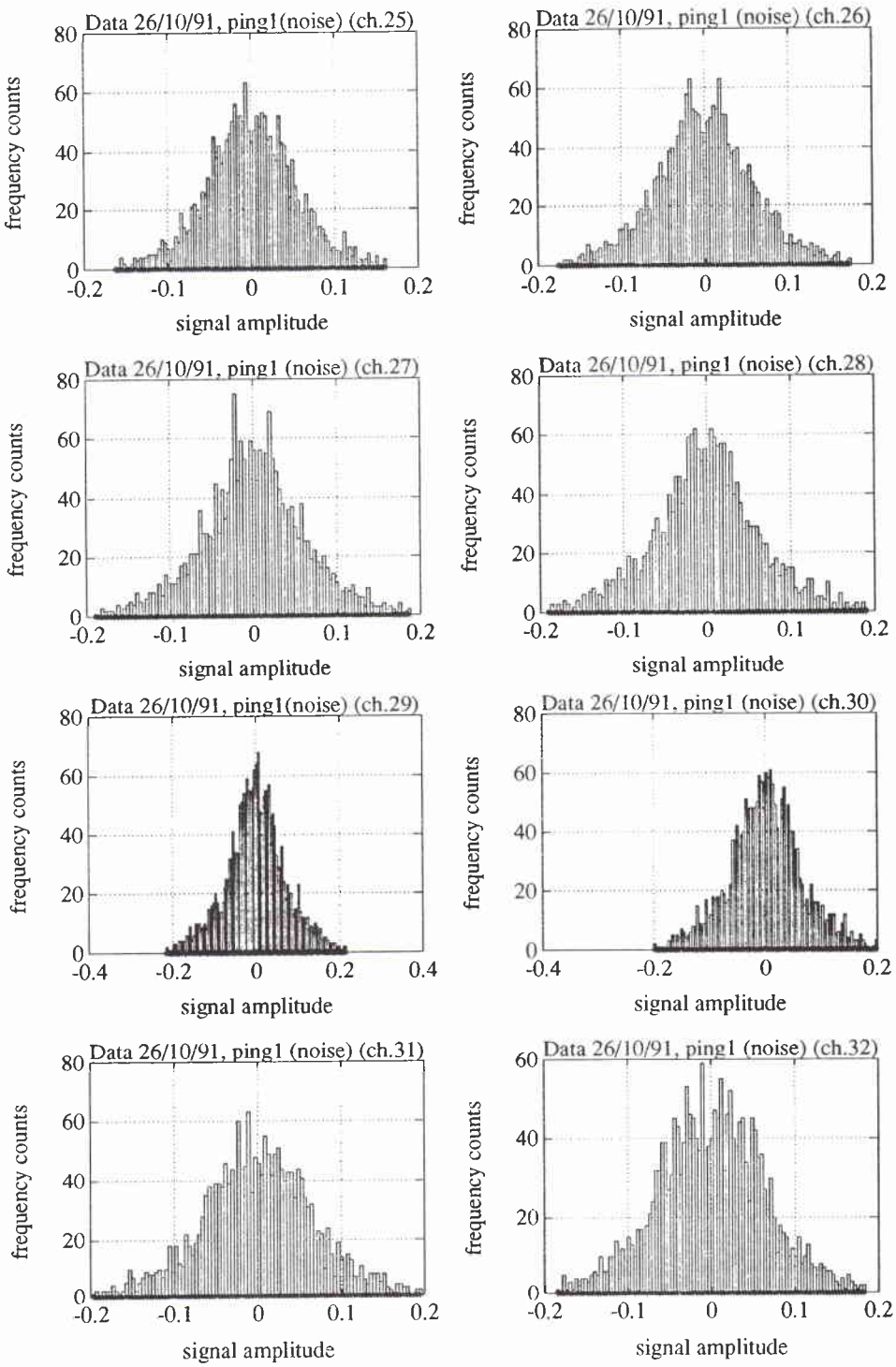

Figure 14 (cont'd) *Histograms of samples selected from the noise prevailing part of the outputs of 32 hydrophones during ping1.*

3 Model formulation

A wavefield generated by M wideband sources in the presence of noise is sampled temporally and spatially by a passive array of N ($N > M$) hydrophones with a known arbitrary geometry. The source signals are characterized as zero mean, stationary stochastic processes over the observation interval T_o, bandlimited to a common frequency band with bandwidth B which may be of the same order of magnitude as the centre frequency f_0. The source signal vector $\mathbf{s}(t)$ may be defined as

$$\mathbf{s}(t) = [s_1(t), \ldots, s_M(t)]^T, \tag{8}$$

where 'T' denotes transpose of a vector or a matrix. The signal $x_i(t)$, received at the ith hydrophone, can be expressed as

$$x_i(t) = \sum_{m=1}^{M} a_{im} s_m(t + \tau_{im}) + n_i(t), \tag{9}$$

where a_{im} is the amplitude response of the ith hydrophone to the mth source, τ_{im} is the propagation time difference between the ith hydrophone and the reference hydrophone and $n_i(t)$ is the additive noise at the ith hydrophone.

The observation interval T_o is divided into K non-overlapping snapshot intervals T_s and for each of these intervals the array output signals $x_i(t)$ are decomposed into J frequency components $x_i(f_j)$, $j = 1, \ldots, J$, via fast Fourier transform (FFT). So, essentially, we sample K times each frequency component of the output signals, thus obtaining the data set $x_k(f_j)$, $j = 1, \ldots, J$; $k = 1, \ldots, K$. From Eq. (9), $x_i(f_j)$ will be given by

$$xi(f_j) = \sum_{m=1}^{M} a_{im} e^{i2\pi f_j \tau_{im}} s_M(f_j) + n_i(f_j), \tag{10}$$

where $s_M(f_j)$ and $n_i(f_j)$ are the jth frequency components of $s_m(t)$ and $n_i(t)$ respectively. We define

$$\mathbf{x}(f_j) \equiv [x_1(f_j), \ldots, x_N(f_j)]^T, \tag{11}$$

$$\mathbf{s}(f_j) \equiv [s_1(f_j), \ldots, s_M(f_j)]^T, \tag{12}$$

$$\mathbf{n}(f_j) \equiv [n_1(f_j), \ldots, n_N(f_j)]^T. \tag{13}$$

Based on the above definitions Eq. (10) can be written, in vector-matrix notation, as

$$\mathbf{x}(f_j) = \mathbf{A}(f_j)\mathbf{s}(f_j) + \mathbf{n}(f_j), \tag{14}$$

where $\mathbf{A}(f_j)$ is the $N \times M$ direction matrix at frequency f_j and is given by

$$\mathbf{A}(f_j) = \begin{pmatrix} a_{11}e^{i2\pi f_j \tau_{11}} & \cdots & a_{1M}e^{i2\pi f_j \tau_{1M}} \\ \vdots & \cdots & \vdots \\ a_{N1}e^{i2\pi f_j \tau_{N1}} & \cdots & a_{NM}e^{i2\pi f_j \tau_{NM}} \end{pmatrix}, \tag{15}$$

or in terms of vectors,

$$\mathbf{A}(f_j) = [\mathbf{a}(f_j, \theta_1), \ldots, \mathbf{a}(f_j, \theta_M)],$$

where the lth $N \times 1$ vector of delays (phase shifts) $\mathbf{a}(f_j, \theta_l)$, used to steer the array beam towards the direction θ_l, is the direction vector at frequency f_j and is given by

$$\mathbf{a}(f_j, \tau_1) = [a_{11}e^{i2\pi f_j \tau_{11}}, \ldots a_{N1}e^{i2\pi f_j \tau_{M1}}]^{\mathrm{T}}. \tag{16}$$

Since $\mathbf{A}(f_j)$ contains information on the unknown parameter vector $\underline{\theta} = [\theta_1, \ldots, \theta_M]^{\mathrm{T}}$ of the directions of arrival, it can be denoted as $\mathbf{A}(f_j, \underline{\theta})$. For a linear array of omnidirectional hydrophones with the same interelement spacing d, $\mathbf{A}(f_j, \underline{\theta})$ becomes

$$\mathbf{A}(f_j, \underline{\theta}) = \begin{pmatrix} 1 & \cdots & 1 \\ \vdots & \cdots & \vdots \\ e^{i2\pi f_j (d/c)(N-1)\sin\theta_1} & \cdots & e^{i2\pi f_j (d/c)(N-1)\sin\theta_M} \end{pmatrix}, \tag{17}$$

where c is the wave propagation speed and $\underline{\theta}$ is measured from the axis which is perpendicular to the array endfire. The lth direction vector is given now by

$$\mathbf{a}(f_j, \theta_l) = [1, \ldots, e^{i2\pi f_j (d/c)(N-1)\sin\theta_1}]^{\mathrm{T}}. \tag{18}$$

Based on the above notation, the spatial covariance matrix $\mathbf{R}_{\mathbf{x}}(f_j)$ is given by

$$\mathbf{R}_{\mathbf{x}}(f_j) = E[\mathbf{x}(f_j)\mathbf{x}(f_j)^{\mathrm{H}}] = \mathbf{A}(f_j, \underline{\theta})E[\mathbf{s}(f_j)\mathbf{s}(f_j)^{\mathrm{H}}]\mathbf{A}(f_j, \underline{\theta})^{\mathrm{H}} + E[\mathbf{n}(f_j)\mathbf{n}(f_j)^{\mathrm{H}}], \tag{19}$$

where 'H' denotes conjugate transpose. If T_{s} is sufficiently large ($1/B \ll T_{\mathrm{s}}$) at each snapshot, $\mathbf{x}_k(f_j)$, $j = 1, \ldots, J$, $k = 1, \ldots, K$, can be shown to be approximately uncorrelated (Brillinger, 1981). Also, $E[\mathbf{s}_k(f_j)\mathbf{s}_k(f_j)^{\mathrm{H}}] = (1/T_{\mathrm{s}})\mathbf{P}_{\mathrm{s}}(f_j)$, where $\mathbf{P}_{\mathrm{s}}(f_j)$ is the unknown signal spectral density matrix (Brillinger, 1981). Then, Eq. (19) becomes

$$\mathbf{R}_{\mathbf{x}}(f_j) = \frac{1}{T_{\mathrm{s}}}[\mathbf{A}(f_j, \underline{\theta})\mathbf{P}_{\mathrm{s}}(f_j)\mathbf{A}(f_j, \underline{\theta})^{\mathrm{H}} + \sigma_n^2(f_j)\mathbf{P}_n(f_j)], \tag{20}$$

where $\mathbf{P}_n(f_j)$ is the noise spectral density matrix and $\sigma_n^2(f_j)$ is the unknown noise spectral power level. Without loss of generality we may assume that $T_{\mathrm{s}} = 1$. Finally, the sample spatial covariance matrix $\hat{\mathbf{R}}_{\mathbf{x}}(f_j)$, which is an estimate of the true spatial covariance matrix $\mathbf{R}_{\mathbf{x}}(f_j)$, is given by

$$\hat{\mathbf{R}}_{\mathbf{x}}(f_j) = \frac{1}{K}\sum_{k=1}^{K} x_k(f_j)x_k(f_j)^{\mathrm{H}}. \tag{21}$$

where '^' denotes the sample value or the estimate of an entity. It is noted that in the above-described model the covariance matrices are functions of the temporal frequencies f_j, $j = 1, \ldots, J$. Therefore, this model leads to a frequency-domain processing.

3.1. THE BEAMFORMING ALGORITHM – A CLASSICAL APPROACH

The most classical approach to the direction finding problem is the so-called beamforming algorithm (Knight et al., 1981; Monzingo and Miller, 1980; Pridham and Mucci, 1978; Rudnick, 1969). For isotropic uniform arrays it can be regarded as the spatial analog of the Fourier method in spectral analysis and it is, essentially, a delay and sum processor which is steered to different directions in the bearing domain. We define the vector of delays $\mathbf{a}(f_j, \theta)$, used to steer the array beam towards the direction θ, as

$$\mathbf{a}(f_j, \theta) = [e^{i2\pi f_j \tau_1(\theta)}, \ldots, e^{i2\pi f_j \tau_N(\theta)}]^{\mathrm{T}}, \tag{22}$$

where $\tau_i(\theta)$ is the propagation time difference between the reference point and the ith hydrophone for a wavefront impinging from direction θ. The average power at the output of the delay and sum processor at frequency f_j is given by

$$P(f_j, \theta) = E[|\mathbf{a}(f_j, \theta)^{\mathrm{H}} \mathbf{x}(f_j)|^2] = \mathbf{a}(f_j, \theta)^{\mathrm{H}} \mathbf{R}_{\mathbf{x}}(f_j) \mathbf{a}(f_j, \theta), \tag{23}$$

where $\mathbf{R}_{\mathbf{x}}(f_j)$ is the spatial covariance matrix of $\mathbf{x}(f_j)$. In practice, $\mathbf{R}_{\mathbf{x}}(f_j)$ is replaced by the sample spatial covariance matrix $\hat{\mathbf{R}}_{\mathbf{x}}(f_j)$ of the array outputs given in Eq. (21). The locations of the local maxima of the estimated spatial spectrum given by

$$\hat{P}(f_j, \theta) = \mathbf{a}(f_j, \theta)^{\mathrm{H}} \hat{\mathbf{R}}_{\mathbf{x}}(f_j) \mathbf{a}(f_j, \theta), \tag{24}$$

are the estimated directions of arrival of the signals at frequency f_j. An average over frequency will give a broadband beamforming output such as

$$\hat{P}_{\mathrm{Beam}}(\theta) = \frac{1}{J} \sum_{j=1}^{J} \mathbf{a}(f_j, \theta)^{\mathrm{H}} \hat{\mathbf{R}}_{\mathbf{x}}(f_j) \mathbf{a}(f_j, \theta). \tag{25}$$

It can be shown that the resolution of the beamformer is determined, essentially, by the beampattern of the hydrophone array. The beamwidth of the beampattern, defined as the inverse of the array aperture expressed in wavelengths, is the resolution limit for a linear, uniform array. In other words, when signals with angle separation less than one beamwidth impinge on a linear, uniform array, they will not be resolved. Since the received signals are low frequency signals, for the beamforming as well as for the array gain, signal gain and noise gain is used the low frequency part of the array, i.e. the 32 hydrophones spaced at 2 m apart.

Classical beamforming results In order to use the beamforming method described above, the data were grouped in signal and noise data as before. Due to the short duration of the signal, only 512 data samples from the output of each hydrophone

were used. These 512 data samples were grouped in eight snapshots of 64 samples each. Since the sampling frequency $f_s = 3000$ samples/s is several times higher than the highest frequency of the sampled hydrophone outputs, an FFT length of only 64 samples would give a low temporal frequency resolution within the bandwidth of interest which, as we have seen from the computation of the signal and noise spectra above, is between 225 and 275 Hz, approximately. Within this bandwidth, for every snapshot, $J = 33$ temporal frequencies were selected, a beamforming output for every frequency was computed (according to Eq. (21)) and the various beamforming outputs were averaged over the individual frequencies according to Eq. (25). For comparison and consistency, this data scheme was used for all computations in this and subsequent sections.

Figure 15 shows beamforming results for several different pings where only signal samples where used, while Fig. 16 shows results for the noise part of the hydrophone outputs. The positive angles of arrival correspond to surface reflections while the negative ones correspond to bottom reflections. The results are consistent and show that the signal arrivals at the array from two different directions close to the broadside may be interpreted as reflections of the original signal from the surface and bottom respectively. For the various pings used here, these two angles of arrival ranged from $-12°$ to $-10.5°$ and from $5.5°$ to $7°$, approximately. The results for the noise are different, but also consistent, and show that the noise was very directional and arrived from the horizontal or very nearly so. This suggests, taking into consideration also the results from the previous steps of data analysis, that the noise was distant shipping noise (Cavanagh, 1982; Urick, 1983, ch. 7).

An interesting question that one might attempt to answer is the coherence of the array during the experiment, i.e. the actual position of the array (vertically positioned or tilted) and array deformation. As far as deformation is concerned, it is rather difficult to know the exact positions of the hydrophones during the experiment and there cannot be an answer to this question due to the lack of such information coming from the hydrophones. The problem becomes more difficult since the array usually changes position (moves around the vertical) and form, depending on the sea conditions during the experiment. As far as tilt is concerned, the beamforming result with its two estimated angles of arrival $\hat{\theta}_1$ and $\hat{\theta}_2$ suggests the following. Since during the particular experiment there existed a symmetry where the acoustic source was almost at the same depth as the mid-point of the array and, at the same time, at half way the water column, a reasonable estimate of the tilt may be concluded by observing the relative differences of the estimated angles of arrival, i.e. tilt $\approx \frac{1}{2}\left\|\hat{\theta}_1| - |\hat{\theta}_2\right\|$ This may not be an accurate method but there are no standard procedures to estimate tilt. In all cases, the above relative difference gave a tilt of approximately 2–3°, which is reasonable since the array was bottom moored and the sea during the experiment was calm.

3.2. EIGEN-DECOMPOSITION BASED METHODS

The eigen-decomposition based methods or signal-subspace methods as they are often referred to, have their origin in Pisarenko's method (1973). Pisarenko was the first to use the eigenvector which corresponds to the smallest eigenvalue of the spatial covariance matrix, to achieve high resolution frequency estimation. The basic concepts of the eigenstructure are outlined below.

The observation spatial covariance matrix $\mathbf{R}_{\mathbf{x}}(f_j)$ of the $N \times 1$ array output vector $\mathbf{x}(t)$ at frequency f_j is given by

$$\mathbf{R}_{\mathbf{x}}(f_j) = \mathbf{A}(f_j, \underline{\theta})\mathbf{P}_{\mathrm{s}}(f_j)\mathbf{A}(f_j, \underline{\theta})^{\mathrm{H}} + \mathbf{R}_{\mathrm{n}}(f_j), \tag{26}$$

where $\mathbf{P}_{\mathrm{s}}(f_j)$ and $\mathbf{R}_{\mathrm{n}}(f_j)$ are the signal spectral density and noise correlation matrices, respectively. If the noise is a zero mean, complex Gaussian stochastic process, independent from sensor to sensor with power $\sigma_n^2(f_j)$ then $\mathbf{R}_{\mathrm{n}}(f_j) = \sigma_n^2(f_j)\mathbf{I}_N$. Let λ_i and $\mathbf{v}_i$, $i = 1, \ldots, N$, be the eigenvalues and eigenvectors, respectively, of $\mathbf{R}_{\mathbf{x}}(f_j)$. If the angles of arrival $\theta_1, \ldots, \theta_M$ are not identical and the signals are not completely correlated, then the eigenvalues have the following properties (Schmidt, 1978):

1. $$\lambda_1 \geq \lambda_2 \geq \ldots \geq \lambda_M > \lambda_{M+1} = \cdots = \lambda_N = \sigma_n^2, \tag{27}$$

2. The space spanned by the columns of $\mathbf{E}_{\mathrm{s}} = [\mathbf{v}_1, \ldots, \mathbf{v}_M]$ is the same as that spanned by the columns of $\mathbf{A}(f_j, \underline{\theta})$. The column span of $\mathbf{E}_{\mathrm{s}}$ is called signal subspace while that of $\mathbf{E}_{\mathrm{n}} = [\mathbf{v}_{M+1}, \ldots, \mathbf{v}_N]$ is called noise subspace. The noise subspace is orthogonal to the signal subspace, i.e. $\mathbf{E}_{\mathrm{s}}^{\mathrm{H}}\mathbf{E}_{\mathrm{n}} = 0$.

3.2.1. The MUSIC algorithm

By using the aforementioned properties, Schmidt (1978) proposed the multiple signal classification (MUSIC) algorithm which uses the noise subspace (or signal subspace) in order to determine the DOAs as the angles for which the spectrum

$$P_{\mathrm{MU}}(\theta) = \frac{1}{\mathbf{a}(f_j, \theta)^{\mathrm{H}}\mathbf{E}_{\mathrm{n}}\mathbf{E}_{\mathrm{n}}^{\mathrm{H}}\mathbf{a}(f_j, \theta)}, \tag{28}$$

reaches its maxima. The estimated number $\hat{M}$ may be determined, before using the MUSIC algorithm, by applying the Lawley-Bartlett test (see Press, 1982). The performance of the MUSIC algorithm has been tested through simulations and has been compared with the classical and high resolution approaches, by Barabell et al. (1984). It has been shown that the resolution capabilities of MUSIC are significantly better than those of conventional methods.

3.2.2. The Minimum Norm algorithm

The Minimum Norm algorithm which was proposed by Kumaresan and Tufts (1983) is another eigen-decomposition method which has better resolution capabilities than MUSIC. Very briefly, the method may be described as follows. The signal subspace is partitioned as

$$\mathbf{E}_s = \begin{pmatrix} \mathbf{g}_s^T \\ \mathbf{G}_s \end{pmatrix}, \tag{29}$$

where the $1 \times M$ row vector $\mathbf{g}_s^T$ consists of the first elements of the signal subspace. In the Minimum Norm method the aim is to find an $N \times 1$ vector $\mathbf{d}$ which satisfies the following conditions:

1. $\mathbf{E}_s\mathbf{d} = 0$.
2. The first element of $\mathbf{d}$ is set equal to unity.
3. The Euclidean norm of $\mathbf{d}$ is minimum.

The Minimum Norm solution is given by

$$\mathbf{d}_{\min} = \begin{pmatrix} 1 \\ -(1 - \mathbf{g}_s^H\mathbf{g}_s)^{-1}\mathbf{G}_s\mathbf{g}_s^* \end{pmatrix}. \tag{30}$$

The DOAs are determined as the locations of the peaks of the spatial spectrum:

$$P_{MN}(\theta) = \frac{1}{|\mathbf{a}(f_j, \theta)^H\mathbf{d}_{\min}|^2}. \tag{31}$$

The MUSIC and Minimum Norm methods concern arrays of arbitrary geometry. The performance of these two algorithms was studied theoretically by Kaveh and Barabell (1986), who indicate that the Minimum Norm method has a lower resolution threshold.

3.3. COHERENT SIGNAL SUBSPACE METHOD (CSS)

An approach to decorrelate the coherent wideband signals for general arrays, is the coherent signal subspace method (CSS), which was first proposed by Wang and Kaveh (1985). This method is basically a preprocessing which may be applied before the final stage of any algorithmic process for the estimation of the direction of the angle of arrival. The final stage can be any of the narrowband direction finding methods. The CSS method proposes transformation matrices (CSST matrices) $\mathbf{T}(f_j, \underline{\beta})$, $j = 1, \ldots, J$ which satisfy

$$\mathbf{T}(f_j, \underline{\beta})\mathbf{A}(f_j, \underline{\theta}) = \mathbf{A}(f_0, \underline{\theta}), \tag{32}$$

where $\underline{\beta}$ is the vector of preliminary focusing angle estimates. The aim of using the transformation matrices is to align the signal subspaces at temporal frequencies f_j,

$j = 1, \ldots, J$, with the signal subspace at centre frequency f_0. The steps of the CSS algorithm are summarized as follows:

1. Array output sampling, data collection, frequency decomposition (see model formulation section).
2. Preliminary processing. Use the classical beamformer technique to obtain an estimate of the focusing angles.
3. Construction of the transformation matrices $\mathbf{T}(f_j, \beta)$. A particularly simple situation is where all the true angles of arrival are within the neighbourhood of a single angle β. The approximate transformation matrices $\mathbf{T}(f_j, \beta)$ can now be of a diagonal form:

$$\mathbf{T}(f_j, \beta) = \text{diag}\left(\frac{a_1(f_0, \beta)}{a_1(f_j, \beta)}, \ldots, \frac{a_n(f_0, \beta)}{a_n(f_j, \beta)}\right), \tag{33}$$

   where $a_i(f_j, \beta)$ is the ith element of the $N \times 1$ direction vector $\mathbf{a}(f_j, \beta)$ focusing at β.

4. Form the matrices

$$\hat{\mathbf{R}}_{\mathbf{x}}(f_j) = \frac{1}{K} \sum_{k=1}^{K} \mathbf{x}_k(f_j) \mathbf{x}_k(f_j)^{\mathrm{H}}, \tag{34}$$

$$\hat{\mathbf{R}}_{\mathbf{y}} = \frac{1}{J} \sum_{j=1}^{J} \mathbf{T}(f_j, \beta) \hat{\mathbf{R}}_{\mathbf{x}}(f_j) \mathbf{T}(f_j, \beta)^{\mathrm{H}}, \tag{35}$$

   and the matrix $\hat{\mathbf{R}}_{\mathbf{n}}$ given by

$$\hat{\mathbf{R}}_{\mathbf{n}} = \frac{1}{J} \sum_{j=1}^{J} \mathbf{T}(f_j, \beta) \mathbf{R}_{\mathbf{n}}(f_j) \mathbf{T}(f_j, \underline{\beta})^{\mathrm{H}}, \tag{36}$$

   where $\mathbf{R}_{\mathbf{n}}(f_j)$ is the noise spatial covariance matrix with a known structure.

5. Compute the eigenstructure of the matrix pencil $(\hat{\mathbf{R}}_{\mathbf{y}}, \hat{\mathbf{R}}_{\mathbf{n}})$
6. Use any narrowband direction finding method, e.g. MUSIC or Minimum Norm.

Wang and Kaveh (1986, 1987) have shown that the CSS method removes coherence of completely correlated signals. If the signals occupy a certain finite frequency bandwidth and if a sufficiently large sample size is used, the CSS method improves the performance of estimation of the DOAs of the multipath signals. The basic assumption that the high resolution methods make is that the received signals are random. When the received signals are deterministic, i.e. known, as are the test signals, then the spatial covariance matrix is going to be singular, exactly as in the case of perfectly correlated signals. In this case any eigen-decomposition based high resolution method used without preprocessing would not resolve the received

signals. The results in this memorandum show that this is not a problem for the CSS method and that the transformation matrices act in such a way that the transformed spatial covariance matrices are no longer singular and may be used by any eigen-decomposition based high resolution method at the last stage of the algorithm.

Finally, due to the frequency domain processing (FFT of array outputs) and coherent averaging of transformed covariance matrices at individual temporal frequencies, the computational burden of the CSS algorithm is rather heavy for real-time applications. However, the method may be used successfully in situations where higher accuracy and low resolution threshold are more important than real-time applications.

Coherent signal subspace method results For the results of this section, as in the case of the classical beamforming, the spatial covariance matrix given by Eq. (21) was used. Figure 17 shows results where the MUSIC-based CSS method was used with experimental data and Fig. 18 shows results where the Minimum Norm-based CSS was used. Specifically, sampled data from the signal prevailing parts of the first four available pings were used; the signal part was comprised of samples where the presence of signal is obvious while the noise spatial covariance matrix was formed of samples selected from the end of each ping (beginning of next ping) where the absence of signal is obvious. Figures 19 and 20 show the corresponding results, where instead of signal, noise samples were used. In the latter case, samples from a section of the noise prevailing parts of the pings, other than that used for the noise, were selected. The focussing angle was $\beta = 0°$ and its selection was based on the classical beamformer's results which showed a signal arrival activity around the neighbourhood of the array broadside. Since the assumption that the noise samples among the individual hydrophone outputs are spatially uncorrelated – so that the noise spatial covariance matrix is equal to a diagonal matrix – does not hold in practice, the problem of computing the eigenstructure of the matrix pencil $(\hat{\mathbf{R}}_{\mathbf{y}}, \hat{\mathbf{R}}_{\mathbf{n}})$ had to be solved. The reason is that in the case where $\hat{\mathbf{R}}_{\mathbf{n}}$ is singular or close to singular, any algorithm that performs singular value decomposition in the above generalized form does not converge. The problem was solved by using the well known diagonal loading method by slightly perturbing $\hat{\mathbf{R}}_{\mathbf{n}}$'s diagonal so that the new matrix pencil was $(\hat{\mathbf{R}}_{\mathbf{y}}, \hat{\mathbf{R}}_{\mathbf{n}} + \delta\mathbf{I}_N)$ where $\mathbf{I}_N$ is an $N \times N$ identity matrix and δ is a small number usually selected to be the arithmetic mean of the smallest eigenvalues of $\hat{\mathbf{R}}_{\mathbf{n}}$. This helped in computing the eigenvalues which were subsequently used in the decision about the number of arriving signals. In our case, two eigenvectors, corresponding to the two largest significant eigenvalues, were used in the formation of the signal subspace. Higher dimension signal subspaces tend to increase the false peaks. The results in which the MUSIC-based CSS was used are in agreement with the classical beamformer's results and, in addition, the sidelobes are suppressed. The results in which the Minimum Norm-based CSS was used, as expected, also show similar results. It appears that the signal arriving from a positive direction close to the broadside is de-emphasized (lower peak) relative to a more distant positive arrival. This is due to the sensitivity of the coherent signal subspace method on the selection of the focussing angle β but, the selection $\beta = 0°$

seems to be the best for the given situation.

The results mentioned above show that the CSS method performs well even with experimental data involving deterministic signals. The results obtained with it are correct since they compare well with the classical beamformer's results. In terms of resolution performance a comparison between the two methods would not be applicable here. Given the fact that the beamwidth of the array is quite narrow and thus the array's natural resolution capability, which is represented by that of the classical beamformer, is already high, then the classical beamformer is adequate to resolve the arrivals of the single existing source's signal with its bottom and surface reflections. So it was expected that the use of the high resolution methods would not reveal more arrivals. However, the fact that the method works with deterministic experimental data, together with its resolution potential make it a good candidate algorithm for use in more complicated situations where more sources are involved.

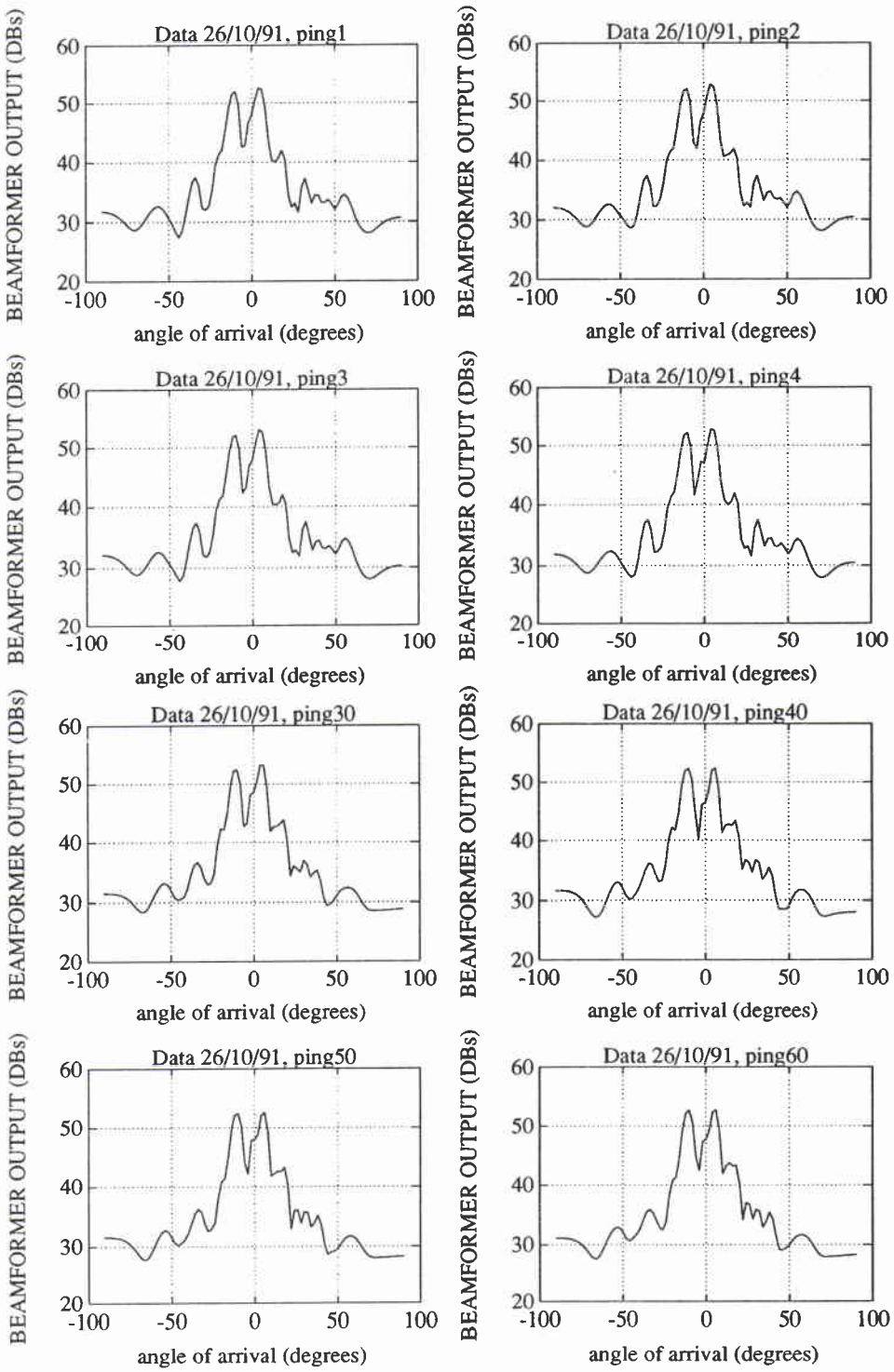

Figure 15 *Classical beamformer outputs of the low frequency part of the array (32 hydrophones). The samples were selected from the signal prevailing part of the pings.*

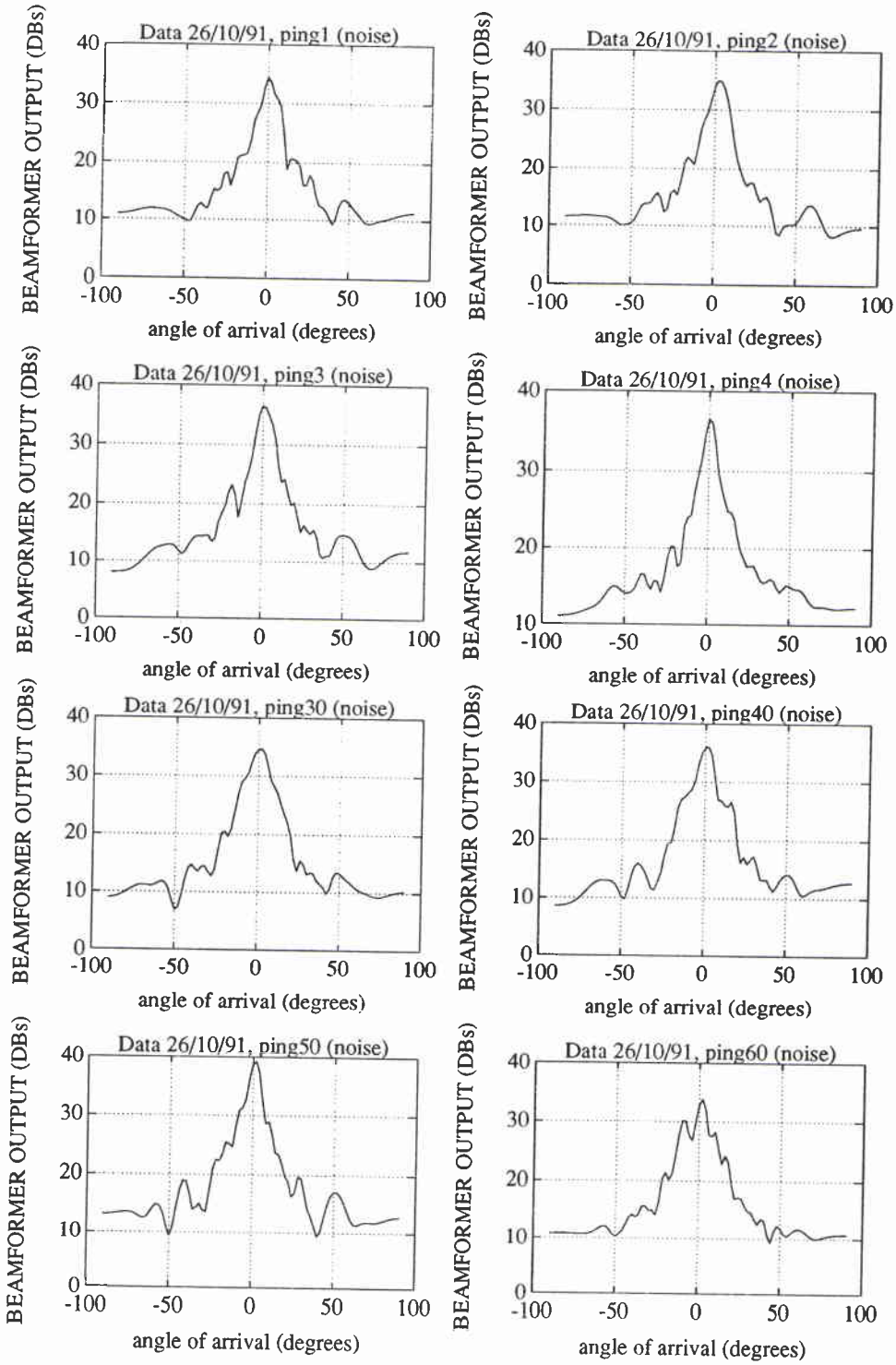

Figure 16 *Classical beamformer output of the low frequency part of the array (32 hydrophones). The samples were selected from the noise prevailing part of the pings.*

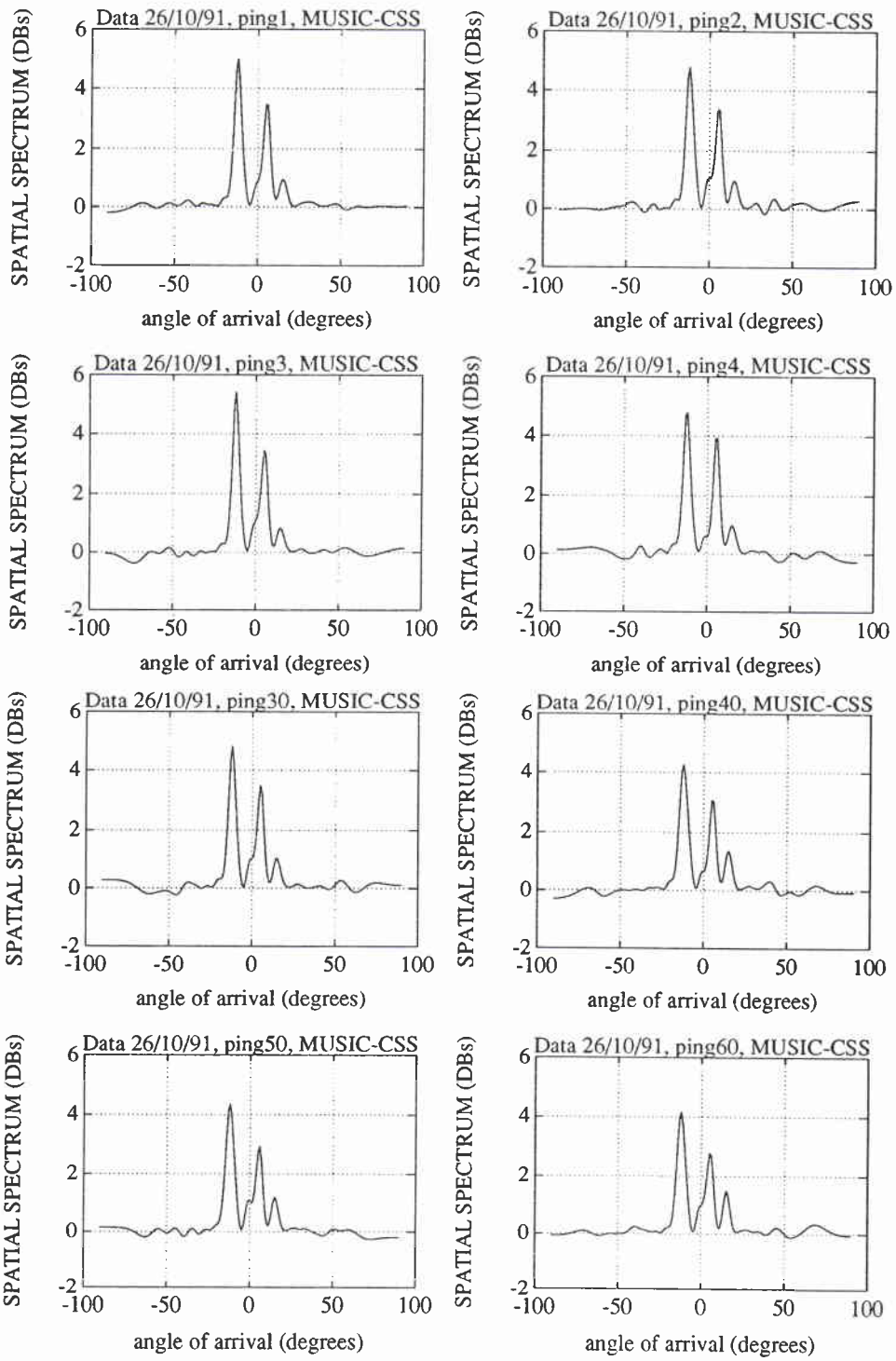

Figure 17 *Signal angle of arrival estimation with* MUSIC*-based coherent signal subspace (CSS) method.*

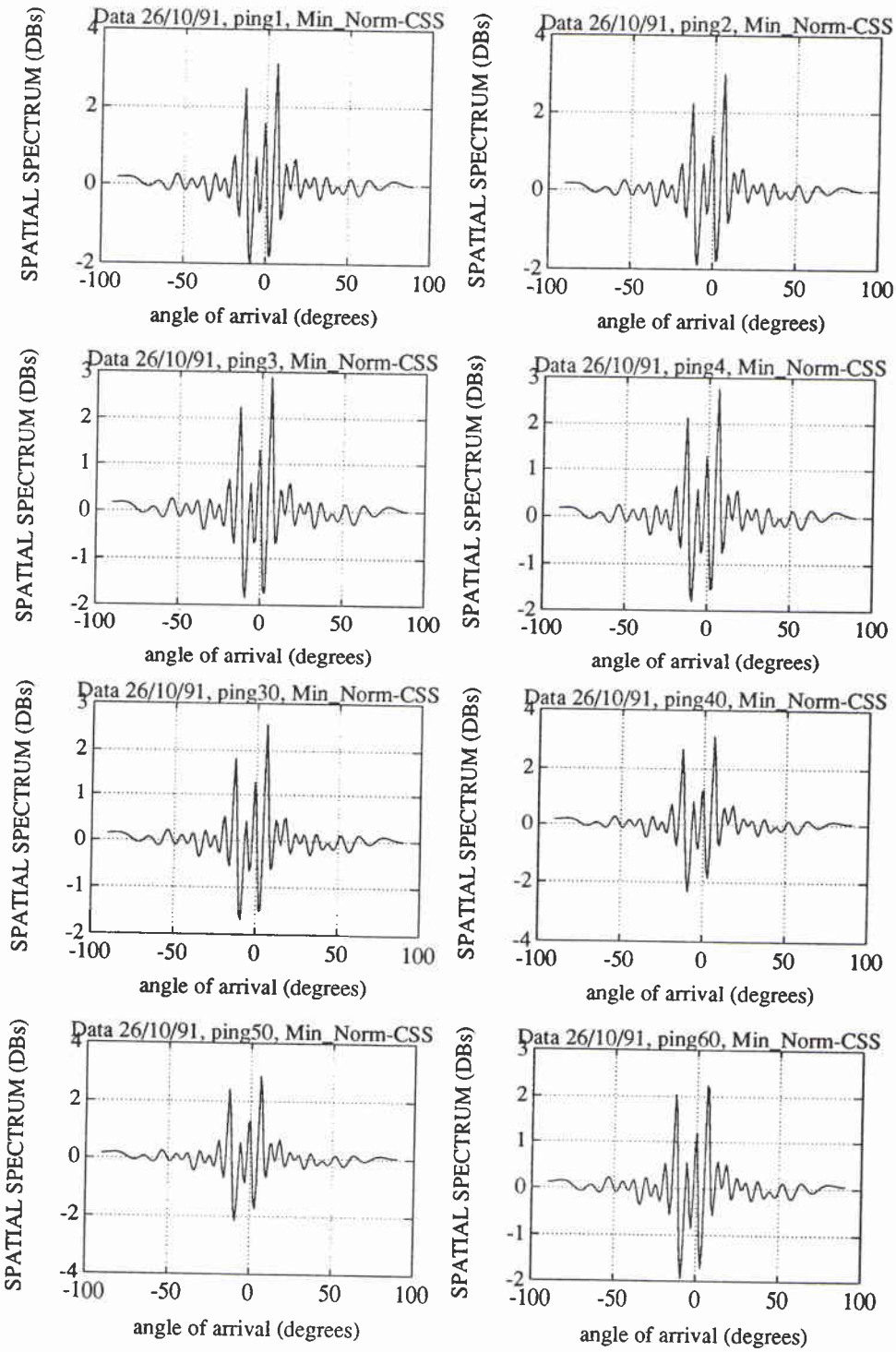

Figure 18 *Signal angle of arrival estimation with Minimum Norm-based coherent signal subspace (CSS) method.*

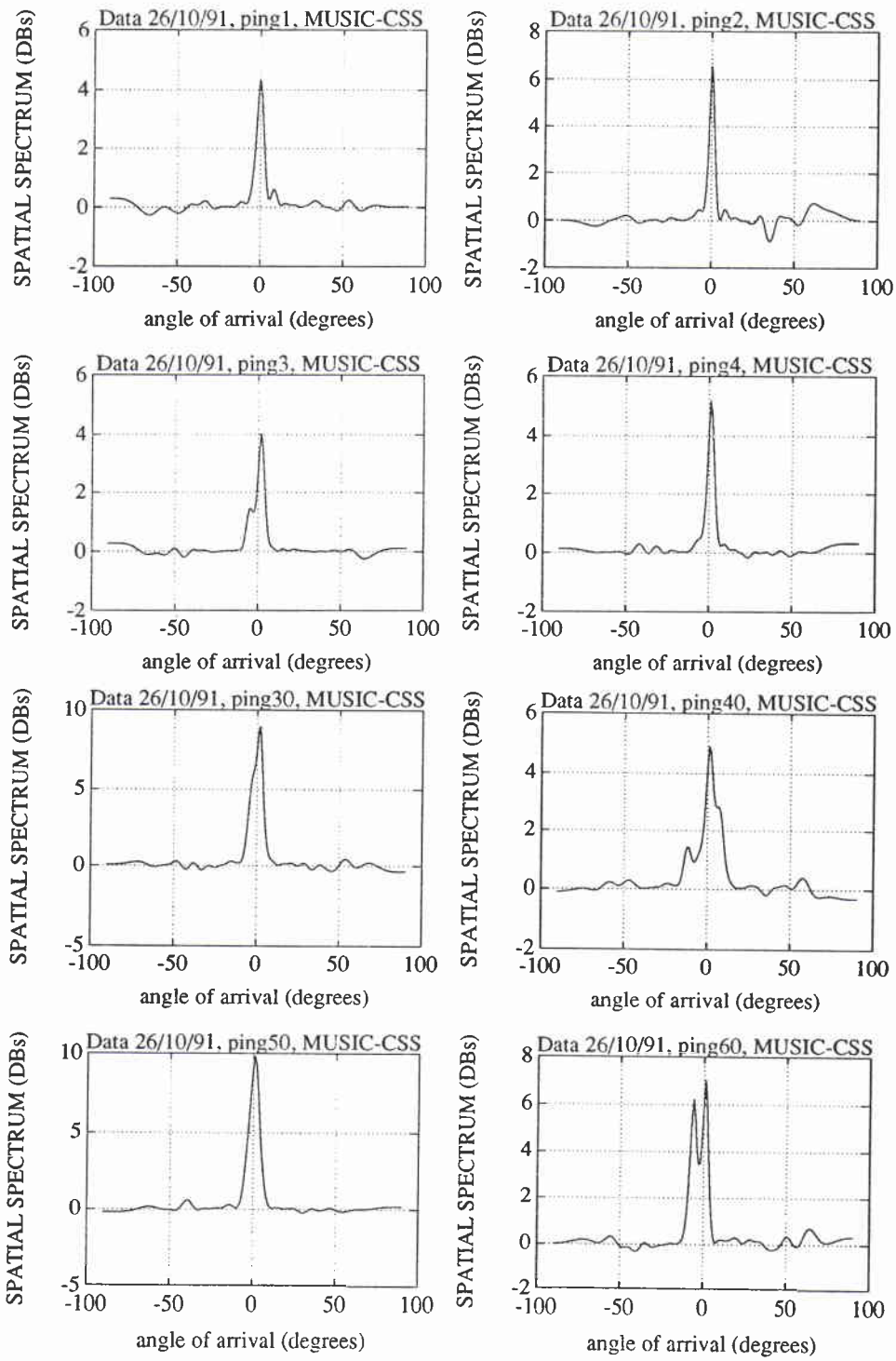

Figure 19 *Noise angle of arrival estimation with* MUSIC*-based coherent signal subspace (CSS) method.*

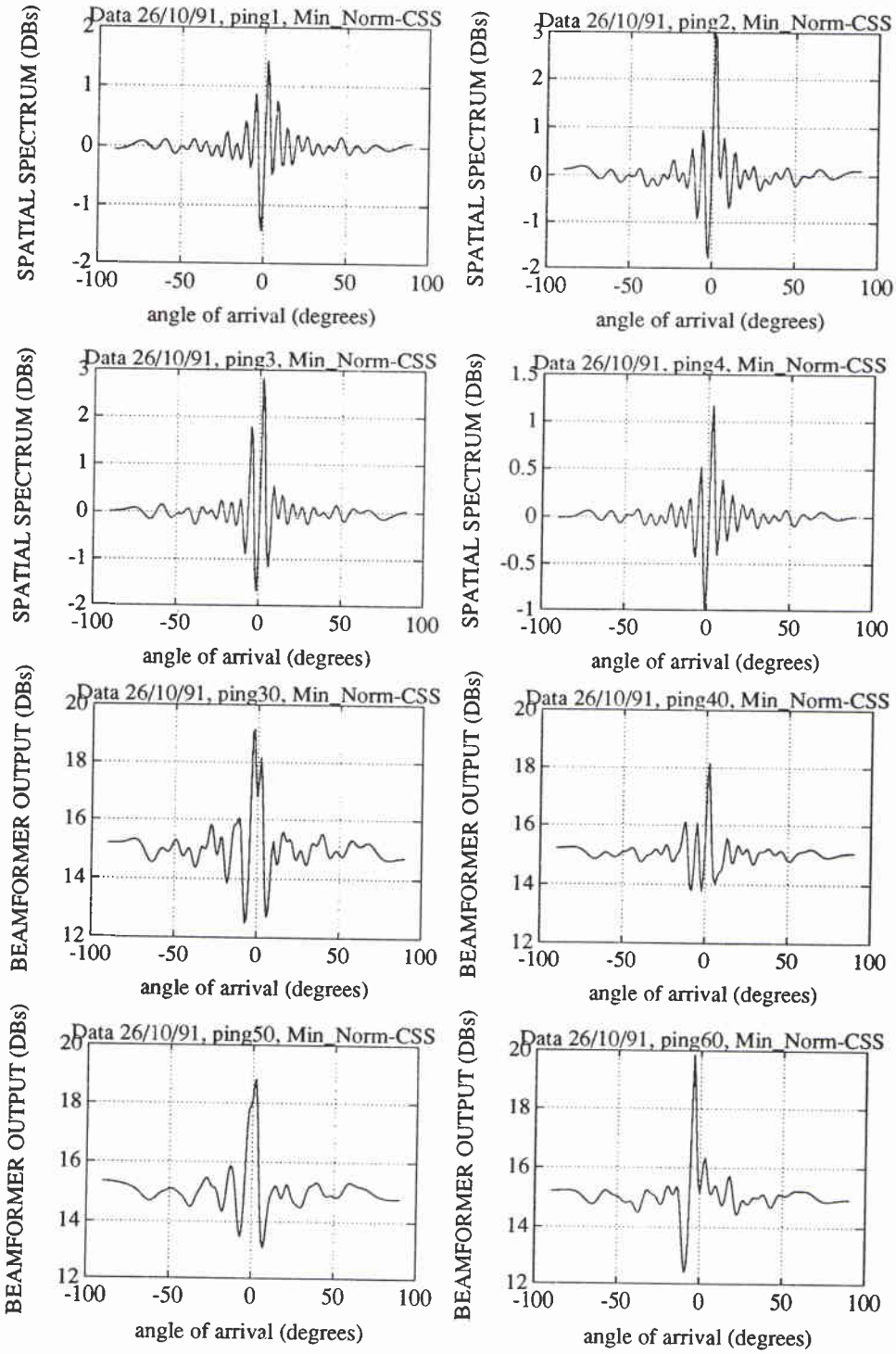

Figure 20 *Noise angle of arrival estimation with Minimum Norm-based coherent signal subspace (CSS) method.*

4

Array gain

The array gain is defined (Urick, 1983) as the improvement in the signal-to-noise ratio at the output of the array over the signal-to-noise ratio at one hydrophone output, i.e.

$$\mathrm{AG} = \frac{(\text{signal power/noise power})_{\text{array output}}}{(\text{signal power/noise power})_{\text{one hydrophone}}} . \tag{37}$$

The above quantity varies with the signal and noise fields in which the array is operating, the type of processing that is used in combining the hydrophone signals and the physical characteristics of the array, i.e. length, number of hydrophones and spacings. In order to obtain a single array output according to the definition above, the individual hydrophone outputs were combined using the classical beamformer in the frequency domain. Since the definition of the array gain requires a reference signal-to-noise ratio and since this ratio varies from hydrophone to hydrophone we have chosen to use the average of the signal-to-noise ratios of all the hydrophones of the array as this ratio. Let us consider the signal part $\mathbf{s}(f_j) \equiv [s_1(f_j), \ldots, s_N(f_j)]^{\mathrm{T}}$ and the noise part $\mathbf{n}(f_j) \equiv [n_1(f_j), \ldots, n_N(f_j)]^{\mathrm{T}}$ of the array. Note that the vector $\mathbf{s}(f_j)$ defines the outputs of the sensors when only samples from the part of the data where signal is present are considered and is not the same as that in Eq. (8) where the source signal vector is defined. The signal power output of the array, when delay and steering is performed on the hydrophone outputs, will be

$$P^{\mathrm{s}}_{\mathrm{Beam}}(f_j, \theta) = E[|\mathbf{a}(f_j, \theta)^{\mathrm{H}} \mathbf{s}(f_j)|^2] = \mathbf{a}(f_j, \theta)^{\mathrm{H}} \mathbf{R}_{\mathrm{s}}(f_j) \mathbf{a}(f_j, \theta) . \tag{38}$$

The average hydrophone signal power is given by

$$P^{\mathrm{s}}_{\mathrm{hyd}}(f_j) = \frac{1}{N} \sum_{i=1}^{N} s_i(f_j)^2) = \frac{1}{N} \|\mathbf{s}(f_j)\|^2 . \tag{39}$$

Similarly, for the noise part the array output power will be given by

$$P^{\mathrm{n}}_{\mathrm{Beam}}(f_j, \theta) = E[|\mathbf{a}(f_j, \theta)^{\mathrm{H}} \mathbf{n}(f_j)|^2] = \mathbf{a}(f_j, \theta)^{\mathrm{H}} \mathbf{R}_{\mathrm{n}}(f_j) \mathbf{a}(f_j, \theta) , \tag{40}$$

while for the average noise power at one hydrophone will be given by

$$P^{\mathrm{n}}_{\mathrm{hyd}}(f_j) = \frac{1}{N} \sum_{i=1}^{N} n_i(f_j)^2 = \frac{1}{N} \|\mathbf{n}(f_j)\|^2 , \tag{41}$$

where $\|\cdot\|$ indicates the norm of a vector. In the above equations (38)–(41) the spatial covariance matrices may be replaced by their estimated value which is computed

using Eq. (21). The above powers may be summed up for the various frequencies f_j; $j = 1, \ldots, J$ within the bandwidth of interest and thus obtain an average, i.e.

$$\bar{P}^{\mathrm{s}}_{\mathrm{Beam}}(\theta) = \frac{1}{J}\sum_{j=1}^{J} P^{\mathrm{s}}_{\mathrm{Beam}}(f_j,\theta) = \frac{1}{J}\sum_{j=1}^{J} \mathbf{a}(f_j,\theta)^{\mathrm{H}}\hat{\mathbf{R}}_{\mathrm{s}}(f_j)\mathbf{a}(f_j,\theta))\,, \tag{42}$$

$$\bar{P}^{\mathrm{s}}_{\mathrm{hyd}}(\theta) = \frac{1}{JN}\sum_{i=1}^{N} \|\mathbf{s}(f_j)\|^2), \tag{43}$$

$$\bar{P}^{\mathrm{n}}_{\mathrm{Beam}}(\theta) = \frac{1}{J}\sum_{j=1}^{J} P^{\mathrm{n}}_{\mathrm{Beam}}(f_j,\theta) = \frac{1}{J}\sum_{j=1}^{J} \mathbf{a}(f_j,\theta)^{\mathrm{H}}\hat{\mathbf{R}}_{\mathrm{n}}(f_j)\mathbf{a}(f_j,\theta))\,, \tag{44}$$

$$\bar{P}^{\mathrm{n}}_{\mathrm{hyd}}(\theta) = \frac{1}{JN}\sum_{j=1}^{J} \|\mathbf{n}(f_j)\|^2)\,. \tag{45}$$

Combining Eqs. (42)–(45) the array gain $\mathrm{AG}(\theta)$ becomes

$$\mathrm{AG}(\theta) = \frac{\bar{P}^{\mathrm{s}}_{\mathrm{Beam}}(\theta)/\bar{P}^{\mathrm{n}}_{\mathrm{Beam}}(\theta)}{\bar{P}^{\mathrm{s}}_{\mathrm{hyd}}(\theta)/\bar{P}^{\mathrm{n}}_{\mathrm{hyd}}(\theta)} \tag{46}$$

or in dBs $\mathrm{AG}(\theta) = \mathrm{SG}(\theta) - \mathrm{NG}(\theta)$, where $\mathrm{SG}(\theta) = 10\log \bar{P}^{\mathrm{s}}_{\mathrm{Beam}}(\theta)/\bar{P}^{\mathrm{s}}_{\mathrm{hyd}}(\theta)$ is the signal gain and $\mathrm{NG}(\theta) = 10\log \bar{P}^{\mathrm{n}}_{\mathrm{Beam}}(\theta)/\bar{P}^{\mathrm{n}}_{\mathrm{hyd}}(\theta)$ is the noise gain.

Using the above analysis the signal and noise gains were computed for directions $\theta \in [-90°, 90°]$ and were compared to the theoretical beampattern. Figures 21 and 22 show the signal and noise gains, respectively, for several pings. It is obvious that the noise gain is high in the spatial area around the broadside. This was expected since the beamforming results have already shown the high directivity of the noise in this spatial area. Bearing this in mind, and also the fact that the array gain, in terms of decibels, is expressed as the difference between the signal and noise gains, it may be concluded that it is not useful to compute and plot the array gain. The reason is that the outcome would be a very small, or even negative, gain in the spatial area in the neighbourhood of the broadside. Therefore, it is better to use the signal gain rather than the array gain as a measure of the performance of the array. More specifically, a good measure of the performance of the array is the computation of the maximum signal gain for various numbers of hydrophones and its comparison with the theoretical gain $20\log N$ for plane waves (see Appendix A), where N assumes values from 1 to 32. Figure 23 shows this comparison for several different pings. It can be seen that the signal gain remained close to the theoretical gain (within 2–4 dB) and this is a good indication that the array performed as expected.

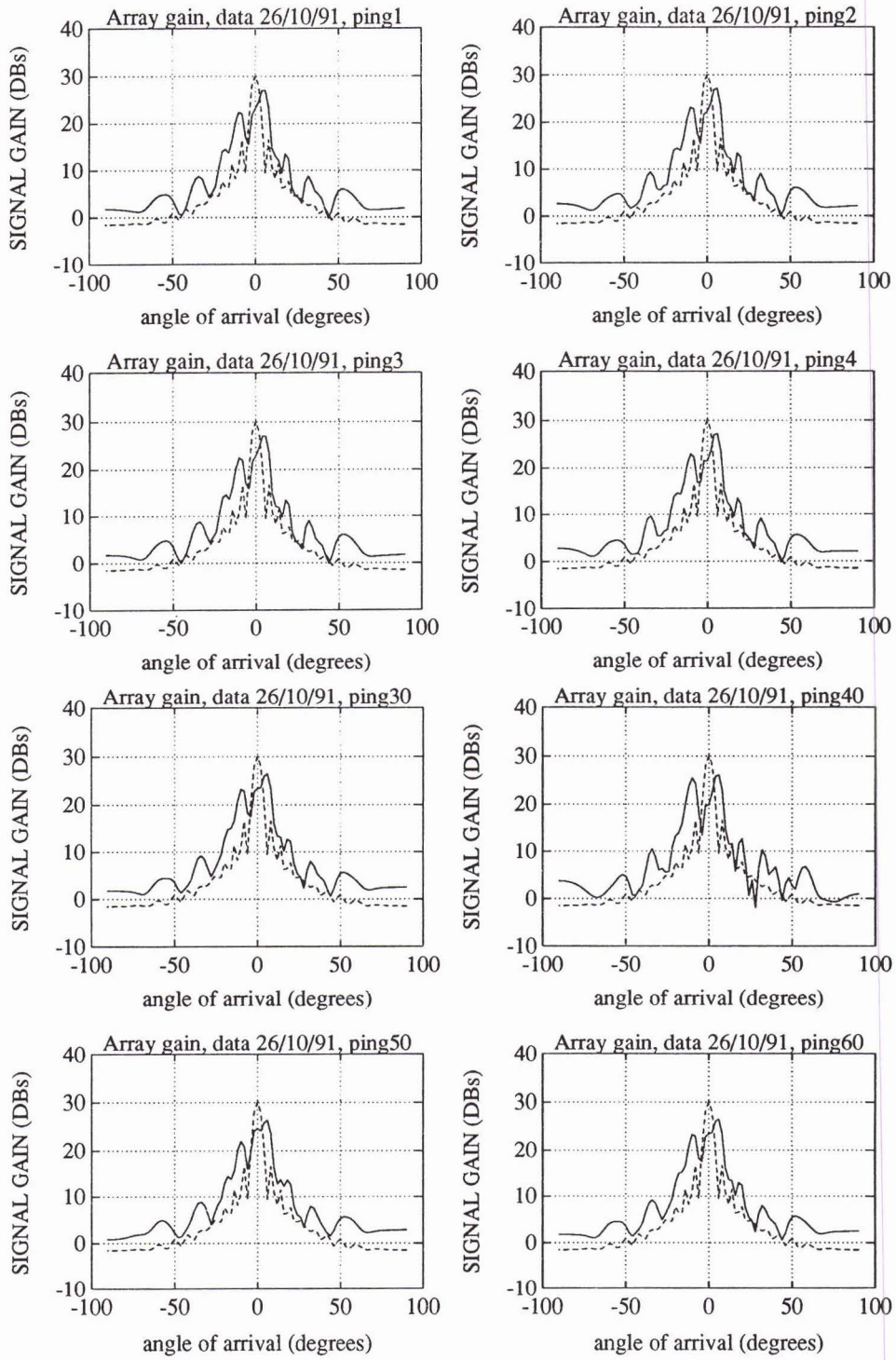

Figure 21 *Signal gain (continuous line) of the low frequency part of the array compared against the theoretical array gain steered at 0°. The samples for the signal gain were selected from the signal prevailing part of the pings.*

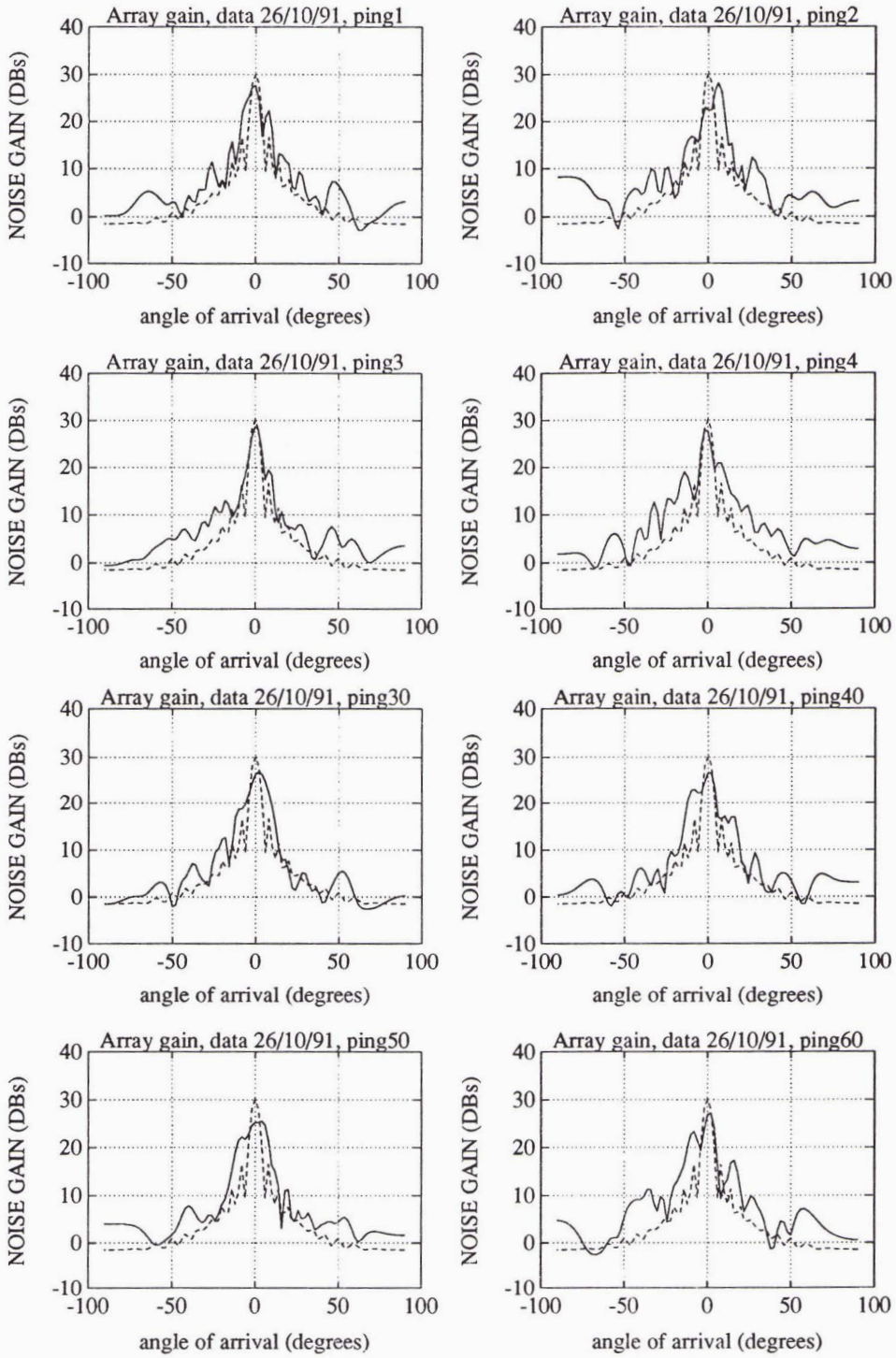

Figure 22 *Noise gain (continuous line) of the low frequency part of the array compared against the theoretical array gain steered at 0°. The samples for the noise gain were selected from the noise prevailing part of the pings.*

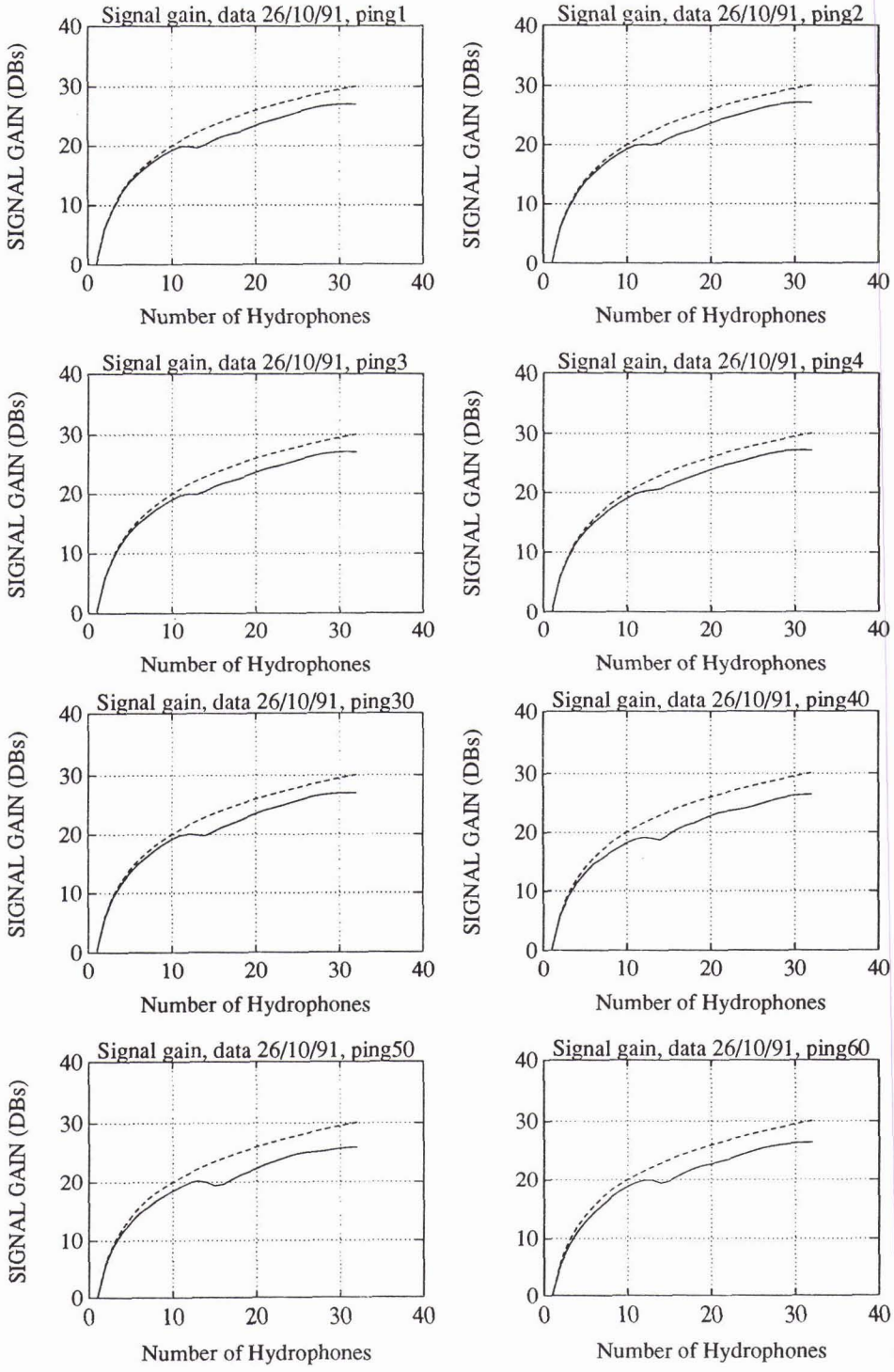

Figure 23 *Comparisons, for various pings, of the maximum signal gain (continuous line) with the maximum theoretical array gain* ($20 \log N$) *vs number of hydrophones.*

5 Conclusions

In this study, a series of measures were used, not only for the assessment of the SACLANTCEN vertical array used during the October–November 1991 sea trials, but also for the evaluation of the quality of the collected data. The measures have been presented, wherever possible, mathematically along with all the underlying assumptions. For the purpose of beamforming, a model based on the assumption of plane waves for the received signals was developed. This assumption may not correspond exactly to the physical reality but does not prevent fairly good estimates of the number of signals and their angles of arrival being obtained. Based on the available information about the exact conditions of the experiment, we have seen that these results cannot be far from reality. As beamformers were used the classical beamformer as well as the MUSIC and minimum norm-based coherent signal subspace algorithm, all in the frequency domain. The above results have also shown that the noise received by the array, has high auto-correlation and cross-correlation, among different hydrophone outputs, and also high directivity which is attributed to distant shipping. This, together with the high noise gain that it produced in a certain narrow spatial area, oriented the study of the performance of the array towards the signal gain which was found to be close to that theoretically predicted for plane waves. The latter, together with all the previously studied measures, leads to the conclusion that the array performed as expected.

References

Anderson V.C., 1979. Variation of the vertical directionality of noise with depth in the North Pacific. *Journal of the Acoustical Society of America*, **66**, 1446–1452.

Barabell, A.J., Capon, J., DeLong, D.F., Johnson J.R. and Senne, K.D., 1984. Performance comparisons of super-resolution array processing algorithms, Project Report TST-72. Lincoln Laboratory.

Bendat, J.S. and Piersol, A.G., 1986. Random Data: Analysis and Measurement Procedures, 2nd edition. New York, NY, Wiley. [ISBN 0 471 0400 2]

Brillinger, D.R., 1988. Time Series: Data Analysis and Theory, 1st edition. New York, NY, McGraw-Hill. [ISBN 0 07 007852 1]

Buckingham, M.S. and Jones, S.A.S., 1987. A new shallow-ocean technique for determining the critical angle of the seabed from the vertical directionality of the ambient noise in the water column. *Journal of the Acoustical Society of America*, **81**, 938–946.

Cavanagh, R.C., 1982. Notes on the interpretation of ambient noise statistics. *In*: Wagstaff, R. A. and Bluy, O.Z., *eds.*, Underwater ambient noise. Proceedings of a conference held at SACLANTCEN on 11–14 May 1982, volume 2, unclassified papers, SACLANTCEN CP-32. La Spezia, Italy, NATO SACLANT Undersea Research Centre: pp. 12/1–12/10.

Clay, C.S. and Medwin, H., 1977. Acoustical Oceanography, Principles and Applications. New York, NY, Wiley, 1977. [ISBN 0 471 16041 5]

Hamson, R.M., 1979. The theoretical response of a passive vertical array in shallow water, SACLANTCEN SM-127. La Spezia, Italy, NATO SACLANT Undersea Research Centre.

Hamson, R.M., 1980. The theoretical gain limitations of a passive vertical line array in shallow water. *Journal of the Acoustical Society of America*, **68**, 156–164.

Hodgkiss, W.S. Jr. and Fisher, F.H., 1990. Vertical directionality of ambient noise at 32 °Nas a function of longitude and wind speed. *IEEE Journal of Ocean Engineering*, **15**, 335–339.

Hollett, R.D., 1992. Observations of underwater sound at frequencies below 1500 Hz from breaking waves at sea, SACLANTCEN SR-183. La Spezia, Italy, NATO SACLANT Undersea Research Centre. Also *Journal of the Acoustical Society of America*, **95**, 1994: 165–170.

Kaveh, M. and Barabell, A.J., 1986. The statistical performance of the MUSIC and the minimum norm algorithms in resolving plane waves in noise. *IEEE Transactions on Acoustics, Speech and Signal Processing*, **34**, 331–341.

Knight, W.C., Pridham, R.C. and Kay, S.M., 1981. Digital signal processing for sonar. *Proceedings of the IEEE*, **69**, 1451–1506.

Kumaresan, R. and Tufts, D., 1983. Estimating the angles of arrival of multiple plane waves. *IEEE Transactions on Aerospace and Electronic Systems*, **19**, 134–139.

Monzingo, R.A. and Miller, T.W., 1980, Introduction to Adaptive Arrays. New York, NY, Wiley. [ISBN 0 471 05744 4]

Oppenheim, A.V. and Schafer, R.W., 1975. Digital Signal Processing. Englewood Cliffs, NJ, Prentice Hall.

Pisarenko, V.F., 1973. The retrieval of harmonics from a covariance function. *Geophysical Journal of the Royal Astronomical Society*, **33**, 347–366.

Press, S.J., 1982. Applied Multivariate Analysis, 2nd edition. Malabar, FL, Krieger.

Pridham, R.G. and Mucci, R.A., 1978. A novel approach to digital beamforming. *Journal of the Acoustical Society of America*, **63**, 425–434.

Rudnick, P., 1969. Digital beamforming in the frequency domain. *Journal of the Acoustical Society of America*, **46**, 1089–1090.

Schmidt, R.O., 1978. Multiple emitter location and signal parameter estimation. *In*: Proceedings of the RADC Spectrum Estimation Workshop held at Griffiss Air Force Base, N.Y., 24–26 May, 1978. Rome Air Development Center, 1978. [AD A 054 650]. Also *IEEE Transactions on Antennas and Propagation*, **34**, 1986: 276–280.

Sotirin, B.J. and Hodgkiss, W.S., 1989. Array performance: a methodology of system calibration and noise identification, MPL TM 410. La Jolla, CA, Scripps Institution of Oceanography. [AD A 220 009]

Tyce, R.C., 1982. Depth dependence of directionality of ambient noise in the north Pacific: experimental data and equipment design. *In*: Wagstaff, R.A. and Bluy, O.Z., *eds.*, Underwater ambient noise. Proceedings of a conference held at SACLANTCEN on 11–14 May 1982, volume 2, unclassified papers, SACLANTCEN CP-32. La Spezia, Italy, NATO SACLANT Undersea Research Centre: pp. 9/1–9/16.

Urick, R.J., 1983. Principles of Underwater Sound, 3rd edition. New York, NY, McGraw-Hill. [ISBN 0 07 066087 5]

Wagstaff, R.A., Berrou J.-L. and Cotaras, F., 1982. Use of the towship for assessing towed array performance and analyzing data quality. *Journal of the Acoustical Society of America*, **72**, 983–992.

Wang, H. and Kaveh, M., 1985. Coherent signal-subspace processing for the detection and estimation of angles of arrival of multiple wide-band sources. *IEEE Transactions on Acoustics, Speech and Signal Processing*, **33**, 823–831.

Wang, H. and Kaveh, M., 1986. On the performance of signal-subspace processing, Part I: narrowband systems, *IEEE Transactions on Acoustics, Speech and Signal Processing*, **34**, 1201–1209.

Wang, H. and Kaveh, M., 1987. On the performance of signal-subspace processing, Part II: coherent wideband systems, *IEEE Transactions on Acoustics, Speech and Signal Processing*, **35**, 1583–1591.

intentionally blank page

Appendix A
Array analysis

For the 32 hydrophones spaced at $d = 2$ m apart and for a known average sound speed c_{av}, which in our case (experiment of 26 October 1991) is $c_{\text{av}} = 1517.359$, the array beamwidth BW can be calculated for different frequencies or different wavelengths. Since the received signals have been filtered and they have a spectrum essentially between $f_{\min} = 225$ Hz and $f_{\max} = 275$ Hz with a center frequency $f_{\text{c}} = 250$ Hz, we obtain

$$\text{BW}_{\max} = \frac{\lambda_{\max}}{d(N-1)} = \frac{c_{\text{av}}}{f_{\min} d(N-1)} = 6.232°,$$

$$\text{BW}_{\min} = \frac{\lambda_{\min}}{d(N-1)} = \frac{c_{\text{av}}}{f_{\max} d(N-1)} = 5.1°,$$

$$\text{BW}_{f_{\min}} = \frac{c_{\text{av}}}{f_{\text{c}} d(N-1)} = 5.61°,$$

where $\lambda_{\min} = c_{\text{av}}/f_{\max} = 5.058$ m, $\lambda_{\max} = c_{\text{av}}/f_{\min} = 7.59$ m, and $\lambda_{f_{\text{c}}} = c_{\text{av}}/f_{\text{c}} = 6.07$ m.

For unidirectional plane waves, and therefore perfectly coherent, and for isotropic noise, that is when the noise power per solid angle is the same in all directions, the array gain reduces to the directivity index or directional pattern (Urick, 1983). The directional pattern of the array (which is the relative sensitivity of response to signals for a specified frequency) from various directions θ, may be found considering the term (Monzingo and Miller, 1980)

$$A(f_j, \theta) = \sum_{n=1}^{N} e^{i2\pi f_j (d/c_{\text{av}})(n-1)\sin\theta}. \tag{A.1}$$

The directional pattern or beampattern is then given by

$$G(f_j, \theta) = 10 \log |A(f_j, \theta)|^2. \tag{A.2}$$

The beampattern assumes a maximum value when $\theta = 0°$ and becomes $G_{\max} = 20 \log N$ which, for $N = 32$, is $G_{\max} = 30$ dB. A beampattern of the array steered at 0° and averaged over temporal frequencies f_j, $j = 1, \ldots, 33$ where $f_1 = 225$ Hz and $f_{33} = 274$ Hz, is shown in Fig. A1.

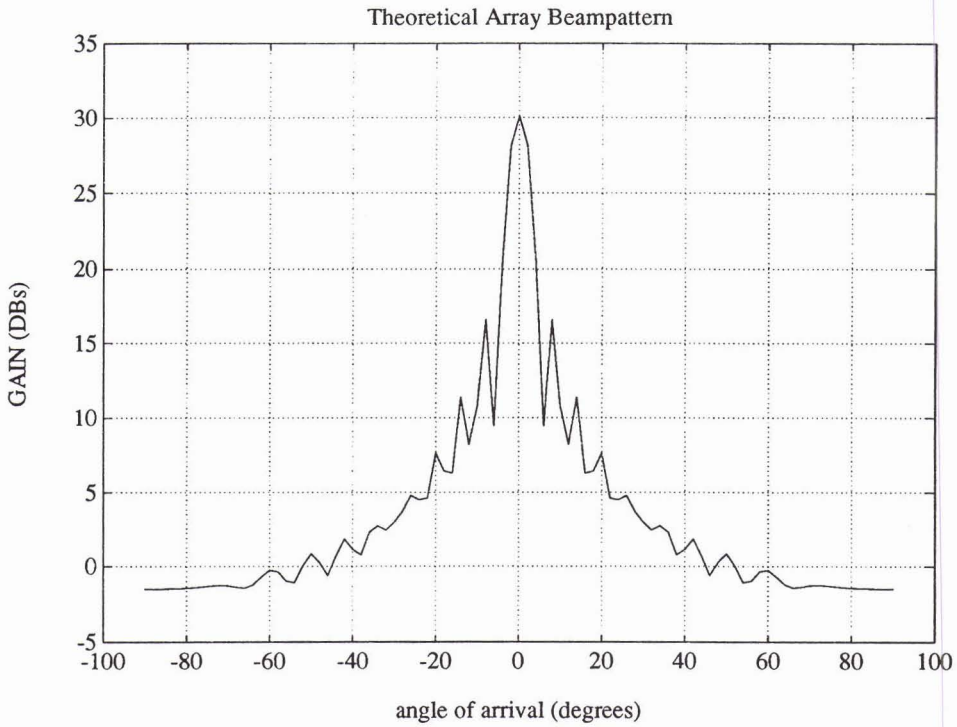

Figure A1 *Beampattern of the low frequency part of the array (32 hydrophones spaced at 2 m), steered at 0° and averaged over temporal frequencies $fj, j = 1, ..., 33$, where $f1 = 225$ Hz and $f33 = 274$ Hz.*

Reportno. changed (Mar 2006): SM-277-UU

Security Classification		Project No.
NATO UNCLASSIFIED		02
Document Serial No.	**Date of Issue**	**Total Pages**
SM-277	March 1994	56 pp.

Author(s)

A. Bassias

Title

Performance assessment of the SACLANTCEN vertical array in shallow water

Abstract

In this memorandum the performance of the SACLANTCEN vertical array is assessed, based on an analysis of experimental data collected in shallow water during the October–November 1991 Signal Processing Group sea trial. The measures that have been used for the assessment of the performance of the vertical array, as well as for the evaluation of the quality of the data, for both the signal and noise fields, seen from both signal processing and statistical points of view, constitute a method that leads to the conclusion whether the array performed as expected. These measures are a survey of the sensors' outputs in the time-domain, computation of spectra both for the signal (plus noise) and purely noise parts, computation of the auto-correlation functions for the sensors' outputs as well as the cross-correlation functions between outputs of selected sensors, and computation of histograms from both signal and noise samples. Furthermore, by treating the received signals at the array – which were test signals – as wideband plane waves, their approximate directions of arrival (DOA) are estimated by using two different methods. The first method is the classical broadband beamforming algorithm and the second method is the coherent signal-subspace (CSS) method, both in the frequency domain. The usefulness (besides the apparent one) of the results of the DOA estimation in the problem of estimating the coherence of the array (vertical or tilted positioning) is discussed. Finally the array gain, based on the experimental data, is computed and compared with the theoretical one as another important measure which is an indicator that the array would be fit for its intended use. The noise field along with its vertical directivity are proven to be decisive factors in the above computation, and therefore in the assessment of the array's performance.

Keywords

array gain, beamforming, coherent signal subspace (CSS), fast fourier transform (FFT), performance assessment, vertical array

Issuing Organization

North Atlantic Treaty Organization
SACLANT Undersea Research Centre
Viale San Bartolomeo 400, 19138 La Spezia, Italy

tel: 0187 540 111
fax: 0187 524 600
telex: 271148 SACENT I

*[From N. America: SACLANTCEN CMR-426
(New York) APO AE 09613]*

Initial Distribution for SM-277

SCNR for SACLANTCEN	
SCNR Belgium	1
SCNR Canada	1
SCNR Denmark	1
SCNR Germany	1
SCNR Greece	1
SCNR Italy	1
SCNR Netherlands	1
SCNR Norway	1
SCNR Portugal	1
SCNR Spain	1
SCNR Turkey	1
SCNR UK	1
SCNR US	2
French Delegate	1
SECGEN Rep. SCNR	1
NAMILCOM Rep. SCNR	1

National Liaison Officers	
NLO Belgium	1
NLO Canada	1
NLO Denmark	1
NLO Germany	1
NLO Italy	1
NLO Netherlands	1
NLO UK	3
NLO US	4

Total external distribution	30
SACLANTCEN Library	20
Total number of copies	50